THE EFFECT OF RIVETED AND UNIFORMLY SPACED STRINGERS ON THE STRESS INTENSITY FACTOR OF A CRACKED SHEET

By

Clarence C. Poe, Jr.

Thesis submitted to the Graduate Faculty of the

Virginia Polytechnic Institute

in candidacy for the degree of

MASTER OF SCIENCE

in

Engineering Mechanics

April 1969

THE EFFECT OF RIVETED AND UNIFORMLY SPACED STRINGERS ON THE STRESS INTENSITY FACTOR OF A CRACKED SHEET

by

Clarence C. Poe, Jr.

Thesis submitted to the Graduate Faculty of the

Virginia Polytechnic Institute

in candidacy for the degree of

MASTER OF SCIENCE

in

Engineering Mechanics

APPROVED:

C. W. Smith

R. A. Heller

H. F. Brinson

April 1969

Blacksburg, Virginia

II. TABLE OF CONTENTS

III. ACKNOWLEDGEMENTS

Acknowledgements are hereby made to Professor C. W. Smith of Virginia Polytechnic Institute for his aid in the preparation of this thesis and to the National Aeronautics and Space Administration for permission to publish the results as a thesis.

IV. LIST OF FIGURES

FIGURE PAGE

FIGURE PAGE

V. INTRODUCTION AND LITERATURE REVIEW

The fail-safe design philosophy which is widely accepted today makes several requirements of a structure. First, the progress of a fatigue crack through a structure must be reasonably slow so as to ensure its discovery. Secondly, the structure containing a crack of detectable length must retain enough static strength to withstand some specified load. Experimental investigations of stiffened sheets containing a fatigue crack have shown that stringers can be effective in reducing crack propagation rates and increasing residual strength. Thus it is important to understand how stringers can be most efficiently used in a fail-safe design and to be able to predict crack propagation rates and residual strength.

A number of investigators have examined the effect of one or two stringers on the stresses in a cracked sheet. Romauldi, Frasier, and Irwin (ref. 1) considered the case of a crack located midway between two riveted stringers. Only the rivets nearest the crack in each stringer were assumed to be effective, and the boundary condition on the crack involving the normal stress was satisfied on the average only. Sanders (ref. 2) considered a continuously attached stringer where the crack extended equally on both sides of the stringer. In the solution the sheet was assumed to be inextensional in the direction parallel to the crack. Isida and Itagaki (ref. 3), assuming the crack to be a thin elliptical hole, considered the problem of two continuously attached stringers with the crack located midway between the stringers.

They also included the bending stiffness of the stringers. Greif and Sanders (ref. 4) considered the same problem as Sanders but obtained the solution for a state of plane stress, thus eliminating the inextensional assumption. They also obtained the solution for a nonsymmetric crack. Isida (ref. 5) considered this same problem but introduced the effect of the bending stiffness of the stringer. For the case of zero-bending stiffness, his solution reduces to that of Greif and Sanders. Isida, Itagaki, and Iida (ref. 6) considered the problem of a sheet with a centrally located crack and continuously attached edge reinforcements. The bending stiffness of the edge reinforcements was also taken into account. Bloom and Sanders (ref. 7) considered the problem of a cracked sheet with a riveted stringer. Solutions were obtained for both a symmetric and a nonsymmetric crack.

In most cases, the designer is concerned with fatigue cracks in tension panels having regularly spaced stringers, where the crack can extend across several bays of stringers. In this thesis the effect of riveted and uniformly spaced stringers on the stresses in a cracked sheet are investigated. The sheet and stringers were assumed to be in a state of plane stress and subjected to a uniform axial strain at infinity normal to the crack. The stringers were treated as straps and assumed to be uniformly spaced, of equal size and shape, and attached to the sheet with rivets of uniform diameter and spacing. The crack was assumed to be located symmetrically with respect to the stringers and pass through a row of rivets. The displacement fields in the straps and sheet were determined as in reference 1 except for

the displacement field in the sheet due to the rivet forces. In determining the latter displacement field in reference 1, the boundary conditions along the crack were satisfied only on the average. In the present solution these boundary conditions are satisfied exactly by using a solution for point forces applied to the crack surface as a Green's function. The effect of the rivet holes on the displacement fields in the sheet and stringer was neglected. The method of consistent displacements was applied to the sheet and stringers resulting in an infinite number of coupled algebraic equations for the rivet forces. The number of stringers and rivets were truncated and the resulting equations solved on a CDC 6600 digital computer.

A stress intensity factor for the stiffened sheet was determined by superimposing the stress intensity factors for the rivet forces and remotely applied stress. The effect of stringer and rivet spacing and size on the stress intensity factor is given by a stress intensity correction factor defined to be the ratio of stress intensity factors of the cracked sheet with and without the stringers. This ratio is equivalent to the "correction factor" in references 2, 4, and 7 and a comparison is shown for the case of one stringer. The rivet forces and stringer loads were also found and are included for the critical stringer and rivet.

VI. SYMBOLS

A_{ij}	displacement in the cracked sheet at the ith rivet due to a force of unity in the jth rivet, in./lbf
A^s_{ij}	displacement in the stringer at the ith rivet due to a force of unity in the jth rivet, in./lbf
a	half crack length, in.
B_i	displacement in the cracked sheet at the ith rivet due to an applied uniaxial stress of unity, in./ksi
B^s_i	displacement in the stringer at the ith rivet due to an applied uniaxial stress of unity, in./ksi
C	stress intensity correction factor
C_1, C_2	functions defined by equation (A-9)
d	rivet diameter, in.
E	Young's modulus for the cracked sheet, ksi
E_s	Young's modulus for the stringers, ksi
K_{st}	stress intensity factor for the stiffened sheet, $\sqrt{\text{in.}}$ ksi
$\bar{K}$	stress intensity factor for the sheet due to a force of unity in the jth rivet, $\sqrt{\text{in.}}$ ksi/lbf
ksi	kilopound per square inch
L	stringer load concentration factor
L_{max}	maximum possible value of L
p	rivet spacing, in.
Q	force in a rivet, lbf
Q_j	force in the jth rivet, lbf

R	maximum force in a stringer, lbf
s	stringer spacing, in.
t	sheet thickness, in.
t_s	stringer thickness, in.
v	y-component of displacement, in.
v_i	displacement in the cracked sheet at the ith rivet, in.
v_i^s	displacement in the stringer at the ith rivet, in.
w	stringer width, in.
x,y	Cartesian coordinates
x_o,y_o	coordinates of the rivet
% stiffening	stiffening parameter, $\dfrac{100}{1 + \dfrac{stE}{wt_sE_s}}$
$\alpha_1,\alpha_2,\alpha_3,\alpha_4$	functions defined in equation (A-7)
β_n	functions defined in equation (B-3)
Γ	function defined in equation (A-9)
θ	function defined in equation (9)
Λ	function defined in equation (A-10)
ν	Poisson's ratio for sheet and stringers
ξ	distance from the origin to a point on the crack, in.
ρ_1,ρ_2	functions defined in equation (A-1)
σ	uniformly applied axial stress, ksi
σ_{xx},σ_{yy}	x and y components of axial stress, ksi
$\bar{\sigma}_{yy}$	axial stress applied to crack surface, ksi
τ_{xy}	shearing stress, ksi

Φ_1, Φ_2	functions defined in equation (9)
ϕ_1, ϕ_2	functions defined in equation (A-1)
ψ	function defined in equation (B-2)
Ω	function defined in equation (A-7)

VII. FORMULATION OF THE PROBLEM

Consider the problem of the cracked sheet with riveted stringers as shown in figure 1. The sheet and stringer are subjected to the uniaxial stresses σ and $\frac{\sigma E_s}{E}$, respectively, so that the strains will be equal at remote distances from the crack. The stringers and rivets are uniform in size and equally spaced, and the crack is contained wholly by the sheet. Figure 2 shows the rivet forces acting symmetrically with respect to the crack and in opposite directions on the sheet and stringer as required by equilibrium. The component of rivet force transverse to the applied stress is secondary and not included here. Isida's results (ref. 5) indicate that the bending stiffness of the stringer is of secondary importance to the axial stiffness of the stringer. A state of plane stress will be assumed in the sheet and stringers.

Let A_{ij} be an influence coefficient which defines the displacement of the ith rivet due to a unit load at the jth rivet and B_i define the displacement of the ith rivet due to an applied uniaxial stress of unity. The displacement of the ith rivet in the cracked sheet due to the unknown rivet forces Q_j and the applied uniaxial stress σ becomes

$$v_i = -\sum_j A_{ij}Q_j + B_i\sigma, \tag{1}$$

where the summation over j includes all the rivets. Using a superscript S to denote stringer, it follows that the displacement of the ith rivet in the stringer becomes

$$v_i^S = \sum_j A_{ij}^S Q_j + B_i^S \frac{E_S}{E} \sigma. \tag{2}$$

Assuming the rivets to be rigid, the displacements at the rivets in the sheet and stringers must be compatible so that

$$v_i = v_i^S, \qquad (i = 1,2,3, \ldots) \tag{3}$$

must be satisfied simultaneously for all rivets. Substituting equations (1) and (2) into (3), and collecting terms,

$$\sum_j (A_{ij} + A_{ij}^S) Q_j - \left(B_i - \frac{E_S}{E} B_i^S \right) \sigma = 0, \qquad (i = 1,2,3, \ldots). \tag{4}$$

The simultaneous-coupled equations (4) are sufficient to determine the unknown rivet forces. Appendices A and B contain the equations, and their development where necessary, for determining the influence coefficients A_{ij}, B_i, A_{ij}^S, and B_i^S for the cracked sheet and stringers, respectively.

The maximum force in the stringer occurs at the intersection of the stringer with the crack and is equal to the applied force plus the sum of the rivet forces,

$$R = \frac{wt_s \sigma E_s}{E} + \sum_j Q_j^m. \tag{5}$$

The superscript m denotes that j is summed over only those rivets in the mth stringer.

For convenience, a stringer load concentration factor L will be defined as the ratio of the maximum force in the stringer to the force applied to the stringer. Thus

$$R = L \frac{wt_s \sigma E_s}{E} \tag{6}$$

and substituting equation (6) into (5) results in

$$L = 1 + \frac{E}{wt_s \sigma E_s} \sum_j Q_j^m. \tag{7}$$

VIII. STRESS INTENSITY FACTOR

The stress intensity factor is a convenient parameter to describe the effect of the stringers on the stresses in the vicinity of the crack tip. Using Westergaard's method for the stress analysis of cracks, the crack tip stress field can be shown to be proportional to the stress intensity factor (ref. 8). These relations are given in figure 3 for the symmetrical case of plane extension (mode I).

The remote applied stress and the symmetrically applied rivet forces produce only an opening mode of deformation of the crack (mode I). The stress intensity factors due to each can therefore be superimposed and will be equal for both crack tips. The stress intensity factor for the cracked sheet with stringers may then be written

$$K_{st} = \sigma\sqrt{a} + \sum_{j} \bar{K}_j Q_j \tag{8}$$

where $\sigma\sqrt{a}$ and $\bar{K}_j Q_j$ are the stress intensity factors for the uniaxial applied stress (ref. 8) and the jth rivet force, respectively. Assuming the rivet forces to be point forces, the stress intensity factor for the symmetrically applied rivet forces equal to unity in figure 4 is given in reference 9 for the case of plane stress as

$$\bar{K} = \frac{\sqrt{a}}{\pi t}\left[(3 + \nu)\Phi_1 - (1 + \nu)\Phi_2\right] \tag{9}$$

where

$$\Phi_1 = \frac{\theta}{\sqrt{(x_o^2 - y_o^2 - a^2)^2 + 4x_o^2y_o^2}},$$

$$\Phi_2 = \frac{\left[(x_o^2 + a^2)y_o^2 + (x_o^2 - a^2)^2\right]\theta^2 + x_o^2y_o^2(x_o^2 + y_o^2 - a^2)}{\theta\left[(x_o^2 - y_o^2 - a^2)^2 + 4x_o^2y_o^2\right]^{3/2}},$$

and

$$\theta = \frac{1}{\sqrt{2}}\left[\sqrt{(x_o^2 - y_o^2 - a^2)^2 + 4x_o^2y_o^2} - (x_o^2 - y_o^2 - a^2)\right]^{1/2}.$$

An error in reference 9 has been corrected in Φ_2 of equations (9).

It will be convenient to define a stress intensity correction factor to be the ratio C of the stress intensity factor for the cracked sheet with stringers to the stress intensity factor without stringers. Thus

$$K_{st} = C\sigma\sqrt{a} \tag{10}$$

and substituting equation (10) into (8), there results

$$C = 1 + \frac{1}{\sigma\sqrt{a}}\sum_j \bar{K}_j Q_j. \tag{11}$$

IX. NUMERICAL SOLUTION

For a cracked sheet of infinite proportions with uniformly spaced stringers, equations (4) represent an infinite set of coupled algebraic equations for the unknown rivet forces. These equations were truncated and solved on a CDC 6600 digital computer using matrix inversion. Preliminary solutions where the number of rivets and stringers were successively increased revealed that equations (4) could be truncated without affecting the computed value of C by more than 1 percent. The truncation procedure used is as follows: only those rivets in the stringers spanning the crack and the first stringer outboard of the crack tip for a distance of 2a from the crack plane were included in the solution. The effect of the rivets outside of this region was negligibly small because of the small force and large distance from the crack tip. Solutions for the longest crack and smallest rivet pitch resulted in 200 unknowns and required approximately 6-1/2 minutes per solution on the computer.

X. RESULTS

Figure 5 shows a comparison of the present results with those of reference 7 for the case of a single riveted stringer. A value of 0.33 was used for Poisson's ratio in all of the present calculations. The results for a continuously attached stringer (ref. 4) are also included and are shown as asymptotes for small values of rivet pitch. Both C and L are shown against a rivet spacing parameter p/a for different values of a stiffening parameter, λ. (Note that the correction factor in references 4 and 7 is identical to the stress intensity correction factor used here.) A value of $p/d = 5.0$ was assumed in the present solution as in reference 7. In addition, a value of $w/d = 1.0$ was chosen to represent the state of uniaxial stress assumed for the stringer in reference 7. The agreement of the results for the riveted stringer is very good with the maximum difference being less than 4 percent. Moreover, both solutions approach the solution for the continuously attached stringer as the value of rivet pitch becomes small.

For multiple stringers, it will be convenient to use a more familiar stiffening parameter "percent stiffening." For regularly spaced stringers of uniform size,

$$\% \text{ stiffening} = \frac{100}{1 + \dfrac{stE}{wt_sE_s}} \tag{12}$$

For $E/E_s = 1$, equation (12) gives the area of the stringers as a percent of the total area of stringers plus sheet. It is important

to note here that the stringer load concentration factor and the force in a single rivet each have a maximum possible value. Consider the limiting case where the crack has progressed entirely through the sheet. Then the force applied to the sheet (σst per stringer) must be transferred to the stringers so that the force in a stringer becomes

$$R = \frac{wt_s E_s \sigma}{E} + \sigma st. \tag{13}$$

From equation (6), the maximum possible value of L becomes

$$L_{max} = 1 + \frac{stE}{wt_s E_s} \tag{14}$$

Substituting equation (12) into (14),

$$L_{max} = \frac{100}{\%\ \text{stiffening}} \tag{15}$$

Thus the stringer load concentration factor can become very large for small values of "% stiffening." Because the force applied to the sheet must be transferred to the stringers through the rivets, the maximum possible force in a single rivet is σst.

In order to present some general observations regarding the effect of multiple stringers, results from the present solution are shown in figure 6 for the case of a crack initiating at a rivet and progressing beneath successive stringers. Some typical values are assumed for the stiffening parameters, 50% stiffening, $s/p = 25$, $p/d = 4.0$, and

w/d = 5.0. In figure 6(a) the effect of the stringers is to reduce the stress intensity factor, that is, $C < 1.0$ which is the value for no stringers. For a very small crack, the stringer has no effect. As the crack increases in length, C is progressively reduced with marked reductions occurring as the crack tip passes beneath a stringer, thus, the undulating appearance of the curve. Without the undulations, the curve appears to have an asymptotic behavior with increasing crack length.

Figure 6(b) shows the stringer load concentration factor for all of the stringers intersected by the crack. The critical or highest loaded stringer is at the crack origin with the adjacent stringers carrying progressively less load. The force in a stringer increases rapidly as the crack tip passes beneath it and asymptotically approaches its maximum possible value, $L_{max} = 2.0$, after the crack tip passes. The broken line indicates that the curve is extrapolated. (A stringer was not included in the analysis until the crack tip was within one bay of the stringer - see section entitled Numerical Solution.) Figure 6(c) shows the rivet forces for the stringer at the crack origin. The force in the rivets diminishes rapidly with distance from the crack. Therefore, only the force in the first four rivets is shown. The rivets on the centerline contained by the crack have zero force due to symmetry. For increasing crack lengths, the rivet forces asymptotically approach a maximum value. The maximum possible load that can be transferred to a stringer is σst. Thus for the longest crack length, the first four

rivets carry 93 percent of this load with the critical rivet carrying 58 percent. Figure 6(d) shows the force in the first rivet of each stringer intersected by the crack. The first rivet in the stringer at the crack origin is the highest loaded and, therefore, the critical rivet. The force in the first rivet of each stringer increases rapidly as the crack tip passes beneath the stringer and asymptotically approaches a common limiting value after the crack tip passes.

Two of the stiffening parameters, rivet diameter and stringer shape, were found to have only a slight effect on the stress intensity correction factor. Figures 7 and 8 show C against a/s for different values of rivet diameter and stringer shape, respectively. Changing the stringer shape involves changing the width of the stringer while keeping the cross sectional area constant. The range in values of both parameters is extensive and yet C changes by less than 12 percent. The small change in C for different values of rivet diameter was also noted in reference 4 for a single riveted stringer.

For the remaining parameters, the results are presented for two locations of the crack and all combinations of

$$\frac{s}{p} = 1.0,\ 1.5,\ 3.0,\ 6.0,\ 12.0$$

$$\%\ \text{stiffening} = 10\%,\ 30\%,\ 50\%,\ 70\%,\ 90\%$$

Values of $p/d = 4.0$ and $w/d = 5.0$ were used in the calculations. Figures 9 and 10 show the stress intensity correction factor C against a/s for the crack initiating at a rivet and between stringers,

respectively. In both cases, the effect of the rivet holes along the line of the crack is neglected. The effect of increasing both s/p and "% stiffening" is to reduce the stress intensity correction factor C. However, the rate of change of C with respect to both s/p and "% stiffening" decreases for larger values of the latter. Thus some optimum values of s/p and "% stiffening" are suggested. For larger values of s/p, corresponding to a continuously attached stringer, the value of C becomes a minimum just after the crack tip passes beneath a stringer. This same result was obtained for the case of a single-riveted stringer in reference 4.

The increase in stringer effectiveness with increasing values of s/p and "% stiffening" is also seen in the curves of L against a/s in figures 11 and 12. The load carried by the critical stringer increases with s/p and approaches its maximum possible value L_{max} with increasing crack length. For larger values of "% stiffening" L approaches L_{max} more rapidly and the curves for different values of s/p tend to converge. Also, for larger values of s/p, there is a distinct break in the curve when the crack tip reaches the adjacent stringer. It is at this point that the adjacent stringer is loaded, and the critical stringer is relieved from acquiring additional load.

Curves showing the critical rivet force against a/s are presented in figures 13 and 14. These results are interesting and important because the critical rivet is historically the weakest element in the stiffened panel. The results show a strong interdependence of the two parameters s/p and "% stiffening." For "10% stiffening," the force

in the critical rivet for a given crack length increases with s/p except for the two largest values of s/p for which the curves intersect. However, as "% stiffening" increases, the curves for the different values of s/p cross one another so that for "90% stiffening" the order of the curves has been inverted and the limiting value of the rivet force decreases with increasing s/p. Therefore, the critical rivet force can be made smaller by increasing s/p and "% stiffening."

Previous results for single stringers (refs. 1-7) have shown unlimited stringer stresses and rivet forces for increasing crack length. However, the present results for uniformly spaced stringers show that the forces in the critical rivet and stringer do not increase without limit for increasing crack length but asymptotically approach limiting values. The effect of increasing the values of s/p and "% stiffening" is to reduce these limiting values of rivet and stringer force and at the same time decrease the stress intensity factor. Also, the stress intensity correction factor is reduced to a minimum when the crack tip is beyond a stringer a small distance. Thus, the stringers can be effective in arresting a crack.

XI. CONCLUSIONS

A stress intensity correction factor C is presented for the problem of a cracked sheet with riveted stringers of uniform size and spacing. This correction factor is defined as the ratio of stress intensity factors for the cracked sheet with and without stringers. Also presented are the forces in the critical rivet and stringer.

Two stiffening parameters, the ratio of stringer to rivet spacing s/p and the percent of area in the stringers "% stiffening," were found to have a significant effect on the stress intensity correction factor. The effect of increasing each of these parameters was to reduce the stress intensity correction factor with minimum values occurring when the crack tip was a small distance beyond a stringer. Thus, stringers can be effective in arresting a crack.

Previous results for a single stringer have shown the force in the stringer and critical rivet to increase continuously without limit for increasing crack length. However, the present results for uniformly spaced stringers show that the forces in the critical rivet and stringer asymptotically approach limiting values for increasing crack length. Most important, increasing the values of s/p and "% stiffening" decrease the limiting values of the forces in the critical rivet and stringer. Therefore, the stress intensity factor and the forces in the critical rivet and stringer can be reduced simultaneously by increasing s/p and "% stiffening."

XII. APPENDIX A

DISPLACEMENT FIELDS FOR A CRACKED SHEET LOADED WITH A UNIFORM AXIAL STRESS AND RIVET FORCES

Uniform Axial Stress

The stress and displacement fields of the uniaxially and uniformly stressed sheet in figure 15 containing a central crack can be obtained using the Westergaard stress function. The y component of displacement at a point (x,y) for a state of plane stress is given in reference 10 as

$$v = \frac{\sigma}{E}\left\{2\sqrt{\rho_1\rho_2}\,\sin\left(\frac{\phi_1 + \phi_2}{2}\right) - (1 + \nu)\frac{y}{\sqrt{\rho_1\rho_2}}\left[x\cos\left(\frac{\phi_1 + \phi_2}{2}\right) + y\sin\left(\frac{\phi_1 + \phi_2}{2}\right)\right]\right\} \tag{A-1}$$

where

$$\rho_1 = \sqrt{(x - a)^2 + y^2}$$

$$\rho_2 = \sqrt{(x + a)^2 + y^2}$$

$$\phi_1 = \tan^{-1}\left(\frac{y}{x - a}\right)$$

and

$$\phi_2 = \tan^{-1}\left(\frac{y}{x + a}\right).$$

Because the remote stress in equation (A-1) is biaxial, a compressive stress, σ, parallel to the crack must be superimposed. The displacements for this stress are

$$v = - \frac{\nu \sigma y}{E}. \tag{A-2}$$

Adding equations (A-1) and (A-2), the displacement field for the cracked sheet with a uniformly applied uniaxial stress can be written

$$v = \frac{\sigma}{E}\left\{2\sqrt{\rho_1\rho_2}\sin\left(\frac{\phi_1+\phi_2}{2}\right) - y - (1-\nu)\frac{y}{\sqrt{\rho_1\rho_2}}\left[x\cos\left(\frac{\phi_1+\phi_2}{2}\right) + y\sin\left(\frac{\phi_1+\phi_2}{2}\right) - \sqrt{\rho_1\rho_2}\right]\right\}. \tag{A-3}$$

The influence coefficient B_i can now be determined from equation (A-3) by letting the stress σ be unity.

Rivet Forces

The displacement field for a cracked sheet with symmetrically applied point forces can be obtained by the addition of the solutions shown in figure 16. Part A gives the displacements in the sheet without a crack. If a crack of length $2a$ is introduced in the sheet, the boundary conditions that must be satisfied on the crack are

$$\sigma_{yy} = \tau_{xy} = 0 \quad \text{for} \quad |x| \leq a \quad \text{and} \quad y = 0.$$

Due to symmetry the shear stress τ_{xy} will be necessarily zero along $y = 0$. The stress that must be removed in part A, shown as $\bar{\sigma}_{yy}$, is

given by σ_{yy} for $|x| \leq a$ and $y = 0$. This can be accomplished by adding to part A the displacement due to a negative $\overline{\sigma}_{yy}$ applied to the crack surface in part B.

The stress and displacement fields for part A in figure 16 can be determined from the solution for a single point force and superposition. The y-component of the stress and displacement fields for a single point force in the y-direction and located at the origin are given by Love in reference 11 for plane stress as

$$v = -\frac{(1+\nu)Q}{4\pi tE}\left[\frac{1}{2}(3-\nu)\ln(x^2+y^2) + (1+\nu)\left(\frac{x^2}{x^2+y^2}\right)\right] \tag{A-4}$$

and

$$\sigma_{yy} = -\frac{(1+\nu)Q}{4\pi t}\left(\frac{y}{x^2+y^2}\right)\left(\frac{3+\nu}{1+\nu} - \frac{2x^2}{x^2+y^2}\right). \tag{A-5}$$

Equation (A-4) cannot be used to calculate the displacement at the origin because of the singularity at $x = y = 0$. In order to circumvent this problem, the point force Q can be distributed over the rivet diameter d. Integrating equation (A-4), the displacement field becomes

$$v = -\frac{(1+\nu)(3-\nu)Q}{16\pi tE}\left\{\left(\frac{2x}{d}+1\right)\ln\left[\left(\frac{2x}{d}+1\right)^2 + \frac{4y^2}{d^2}\right] - \left(\frac{2x}{d}-1\right)\ln\left[\left(\frac{2x}{d}-1\right)^2 + \frac{4y^2}{d^2}\right] + \left(\frac{1-\nu}{3-\nu}\right)\left(\frac{8y}{d}\right)\tan^{-1}\left(\frac{\frac{y}{d}}{\frac{x^2}{d^2}+\frac{y^2}{d^2}-\frac{1}{4}}\right)\right\} \tag{A-6}$$

For $d^2 \ll x^2 + y^2$, equation (A-6) reduces to (A-4). By translating the origin in equation (A-6) so that the point force is located at a point (x_o, y_o) and then using the principle of superposition, the displacement field for the four point forces in part A of figure 16 can be written

$$v = \frac{(1 + \nu)(3 - \nu)Q}{16\pi tE} \Omega \tag{A-7}$$

where

$$\Omega = (\alpha_1 + 1)\ln\left[\frac{(\alpha_1 + 1)^2 + \alpha_4^2}{(\alpha_1 + 1)^2 + \alpha_3^2}\right] - (\alpha_1 - 1)\ln\left[\frac{(\alpha_1 - 1)^2 + \alpha_4^2}{(\alpha_1 - 1)^2 + \alpha_3^2}\right]$$

$$+ (\alpha_2 + 1)\ln\left[\frac{(\alpha_2 + 1)^2 + \alpha_4^2}{(\alpha_2 + 1)^2 + \alpha_3^2}\right] - (\alpha_2 - 1)\ln\left[\frac{(\alpha_2 - 1)^2 + \alpha_4^2}{(\alpha_2 - 1)^2 + \alpha_3^2}\right]$$

$$+ 4\left(\frac{1 - \nu}{3 - \nu}\right)\left\{\alpha_4\left[\tan^{-1}\left(\frac{2\alpha_4}{\alpha_1^2 + \alpha_4^2 - 1}\right) + \tan^{-1}\left(\frac{2\alpha_4}{\alpha_2^2 + \alpha_4^2 - 1}\right)\right]\right.$$

$$\left. - \alpha_3\left[\tan^{-1}\left(\frac{2\alpha_3}{\alpha_1^2 + \alpha_3^2 - 1}\right) + \tan^{-1}\left(\frac{2\alpha_3}{\alpha_2^2 + \alpha_3^2 - 1}\right)\right]\right\}$$

and

$$\alpha_1 = \frac{2(x - x_o)}{d}$$

$$\alpha_2 = \frac{2(x + x_o)}{d}$$

$$\alpha_3 = \frac{2(y - y_o)}{d}$$

$$\alpha_4 = \frac{2(y + y_o)}{d}.$$

Using the same procedure and equation (A-5), the stress field for the four-point forces in part A of figure 16 can be written as

$$\sigma_{yy} = \frac{(1 + \nu)Q}{\pi t d}\left\{\frac{1}{2}\left(\frac{1 - \nu}{1 + \nu}\right)\left(\frac{\alpha_4}{\alpha_1^2 + \alpha_4^2} + \frac{\alpha_4}{\alpha_2^2 + \alpha_4^2} - \frac{\alpha_3}{\alpha_1^2 + \alpha_3^2} - \frac{\alpha_3}{\alpha_2^2 + \alpha_3^2}\right)\right.$$

$$\left. + \alpha_4\left[\left(\frac{\alpha_4}{\alpha_1^2 + \alpha_4^2}\right)^2 + \left(\frac{\alpha_4}{\alpha_2^2 + \alpha_4^2}\right)^2\right] - \alpha_3\left[\left(\frac{\alpha_3}{\alpha_1^2 + \alpha_3^2}\right)^2 + \left(\frac{\alpha_3}{\alpha_2^2 + \alpha_3^2}\right)^2\right]\right\}. \quad \text{(A-8)}$$

Note that equation (A-5) and, hence, equation (A-8) contain a singularity at the point of application of the point force. This singularity was not removed as in the case of equations (A-6) and (A-7) because equation (A-8) will not be used to calculate the stress σ_{yy} in the vicinity of a rivet. The stress $\bar{\sigma}_{yy}$ on the crack boundary that must

be removed in part B of figure 16 can now be obtained from equation (A-8) by setting $y = 0$ and $\alpha_4 = -\alpha_3 = 2y_o/d$. Making these substitutions and letting $x = \xi$,

$$\bar{\sigma}_{yy} = \frac{(1 + \nu)Qy_o}{2\pi t} \Gamma \tag{A-9}$$

where

$$\Gamma = \left(\frac{1 - \nu}{1 + \nu}\right)\left[\frac{1}{(\xi - x_o)^2 + y_o^2} + \frac{1}{(\xi + x_o)^2 + y_o^2}\right]$$

$$+ 2y_o^2\left\{\left[\frac{1}{(\xi - x_o)^2 + y_o^2}\right]^2 + \left[\frac{1}{(\xi + x_o)^2 + y_o^2}\right]^2\right\}.$$

The displacements due to the negative stress $\bar{\sigma}_{yy}$ applied to the crack surfaces in part B of figure 16 can be determined using a solution for point forces applied to the crack surfaces as a Green's function. The displacement at a point (x,y) due to the forces P shown in figure 17 is given in reference 8 as

$$v = \frac{P}{\pi t E} \Lambda \tag{A-10}$$

where

$$\Lambda = \ln\left(\frac{a^2 - \xi^2 + 2\sqrt{a^2 - \xi^2}\sqrt{C_1 + C_2} + 2C_2}{a^2 - \xi^2 - 2\sqrt{a^2 - \xi^2}\sqrt{C_1 + C_2} + 2C_2}\right)$$

$$- \frac{(1 + \nu)y\sqrt{a^2 - \xi^2}}{C_2}\left[\frac{x(x^2 + y^2 - \xi^2)\sqrt{C_2 - C_1} - y(x^2 + y^2 + \xi^2)\sqrt{C_1 + C_2}}{(x^2 - y^2 - \xi^2)^2 + 4x^2y^2}\right]$$

and

$$C_1 = \frac{1}{2}(a^2 + y^2 - x^2)$$

$$C_2 = \sqrt{C_1^2 + x^2y^2}.$$

Letting $P = t\,\bar{\sigma}_{yy}\,d\xi$ in equation (A-10), the displacement at a point (x,y) in part B of figure 16 becomes

$$v = \frac{1}{\pi E}\int_o^a \bar{\sigma}_{yy}\Lambda\, d\xi. \tag{A-11}$$

Substituting equation (A-9) for $\bar{\sigma}_{yy}$,

$$v = \frac{(1 + \nu)Qy_o}{2\pi^2 tE}\int_o^a \Lambda\Gamma\, d\xi. \tag{A-12}$$

Adding equations (A-7) and (A-12), the required displacement field for a cracked sheet with point forces becomes

$$v = \frac{(1 + \nu)Q}{16\pi tE}\left[(3 - \nu)\Omega + \frac{8y_o}{\pi}\int_o^a \Lambda\Gamma\, d\xi\right]. \tag{A-13}$$

The integral in equation (A-13) can be readily evaluated using numerical techniques.

The influence coefficient A_{ij} can be determined from equation (A-13) by letting the rivet force Q be unity.

XIII. APPENDIX B

DISPLACEMENT FIELD FOR A STRINGER LOADED WITH A UNIFORM AXIAL STRESS AND RIVET FORCES

Uniform Axial Stress

The displacement of a point y of the stringer due to the uniaxial stress $\sigma E_s/E$ is given by the simple relationship

$$v = \frac{\sigma y}{E} \tag{B-1}$$

The influence coefficient B_1^s can be determined from equation (B-1) by letting $\sigma E_s/E$ by unity.

Rivet Forces

Figure 18(a) shows a finite width stringer subjected to a pair of point forces. Figure 18(b) shows an infinite sheet subjected to pairs of equal and uniformly spaced point forces which approximate the behavior of the finite width stringer above. The only boundary condition for the finite width strap not satisfied is $\sigma_{xx} = 0$ along $x = \pm w/2$. The displacement of a point $(0,y)$ in figure 18(b) is given by the displacement of a pair of point forces located at $(0,\pm y_o)$ and a series of point forces located symmetrically about the origin at $(\pm nw,\pm y_o)$. The displacement at $(0,y)$ due to a pair of point forces is given by one-half equation (A-7) with $\alpha_1 = \alpha_2 = 0$. Making these substitutions,

$$v = \frac{(1 + \nu)(3 - \nu)Q}{8\pi t_s E_s}\,\psi \tag{B-2}$$

where

$$\psi = \ln\left(\frac{1 + \alpha_4^2}{1 + \alpha_3^2}\right) + 2\left(\frac{1 - \nu}{3 - \nu}\right)\left[\alpha_4 \tan^{-1}\left(\frac{2\alpha_4}{\alpha_4^2 - 1}\right) - \alpha_3 \tan^{-1}\left(\frac{2\alpha_3}{\alpha_3^2 - 1}\right)\right].$$

The displacement at $(0,y)$ due to the series of point forces at (nw,y_o) is given by a series of expressions of equation (A-7) with $\alpha_1 = -\alpha_2 = -2nw/d$. Making these substitutions,

$$v = \frac{(1 + \nu)(3 - \nu)Q}{8\pi t_s E_s} \sum_{n=1}^{\infty} \beta_n \tag{B-3}$$

where

$$\beta_n = \left(1 - \frac{2nw}{d}\right)\ln\left[\frac{\left(1 - \frac{2nw}{d}\right)^2 + \alpha_4^2}{\left(1 - \frac{2nw}{d}\right)^2 + \alpha_3^2}\right] + \left(1 + \frac{2nw}{d}\right)\ln\left[\frac{\left(1 + \frac{2nw}{d}\right)^2 + \alpha_4^2}{\left(1 + \frac{2nw}{d}\right)^2 + \alpha_3^2}\right]$$

$$+ 4\left(\frac{1 - \nu}{3 - \nu}\right)\left\{\alpha_4 \tan^{-1}\left[\frac{2\alpha_4}{\left(\frac{2nw}{d}\right)^2 + \alpha_4^2 - 1}\right] - \alpha_3 \tan^{-1}\left[\frac{2\alpha_3}{\left(\frac{2nw}{d}\right)^2 + \alpha_3^2 - 1}\right]\right\}.$$

Adding equations (B-2) and (B-3), the required displacement at $(0,y)$ is

$$v = \frac{(1 + \nu)(3 - \nu)Q}{8\pi t_s E_s}\left(\psi + \sum_{n=1}^{\infty}{}' \beta_n\right). \tag{B-4}$$

The influence coefficient A_{ij}^s can be determined from equation (B-4) by letting the rivet force Q be unity.

XIV. REFERENCES

1. Romualdi, J. P., Frasier, J. T., and Irwin, G. R.: Crack-Extension-Force Near a Riveted Stiffener. NRL Rept. 4956, October 11, 1957.

2. Sanders, J. L., Jr.: Effect of a Stringer on the Stress Concentration Factor Due to a Crack in a Thin Sheet. NASA TR R-13, 1959.

3. Isida, M., and Itagaki, Y.: Stress Concentration at the Tip of a Central Transverse Crack in a Stiffened Plate Subjected to Tension. Proceedings of the Fourth U.S. National Congress of Applied Mech., vol. 2, 1962, pp. 955-969.

4. Greif, R., and Sanders, J. L.; Jr.: The Effect of a Stringer on the Stress in a Cracked Sheet. J. Appl. Mech., Trans. ASME, March 1965, pp. 59-66.

5. Isida, M.: Effect of a Stringer on the Stress Intensity Factors for the Tension of a Cracked Wide Plate. Dept. of Mech., Lehigh Univ., Bethlehem, Pa., September 1965.

6. Isida, M., Itagaki, Y., and Iida, S.: On the Crack Tip Stress Intensity Factor for the Tension of a Centrally Cracked Strip With Reinforced Edges. Dept. of Mech., Lehigh Univ., Bethlehem, Pa., September 1965.

7. Bloom, J. M., and Sanders, J. L., Jr.: The Effect of a Riveted Stringer on the Stress in a Cracked Sheet. J. Appl. Mech., Trans. ASME, Series E33, 3, September 1966, pp. 561-570.

8. Paris, P. C., and Sih, G. C.: Stress Analysis of Cracks. Fracture Toughness Testing and Its Applications. ASTM Special Technical Publication No. 381, 1964, pp. 30-81.

9. Paris, P. C.: Application of Muskhelishvili's Methods to the Analysis of Crack Tip Stress Intensity Factors for Plane Problems - Part III. Fracture Mechanics Research for the Boeing Airplane,Co., Institute of Research, Lehigh University, Bethlehem, Pa., 1960.

10. Westergaard, H. M.: Bearing Pressures and Cracks. J. Appl. Mech., 6, A-49, 1939.

11. Love, A. E. H.: A Treatise on the Mathematical Theory of Elasticity. New York, Dover, 4th Ed., 1944, p. 209.

The vita has been removed from the scanned document

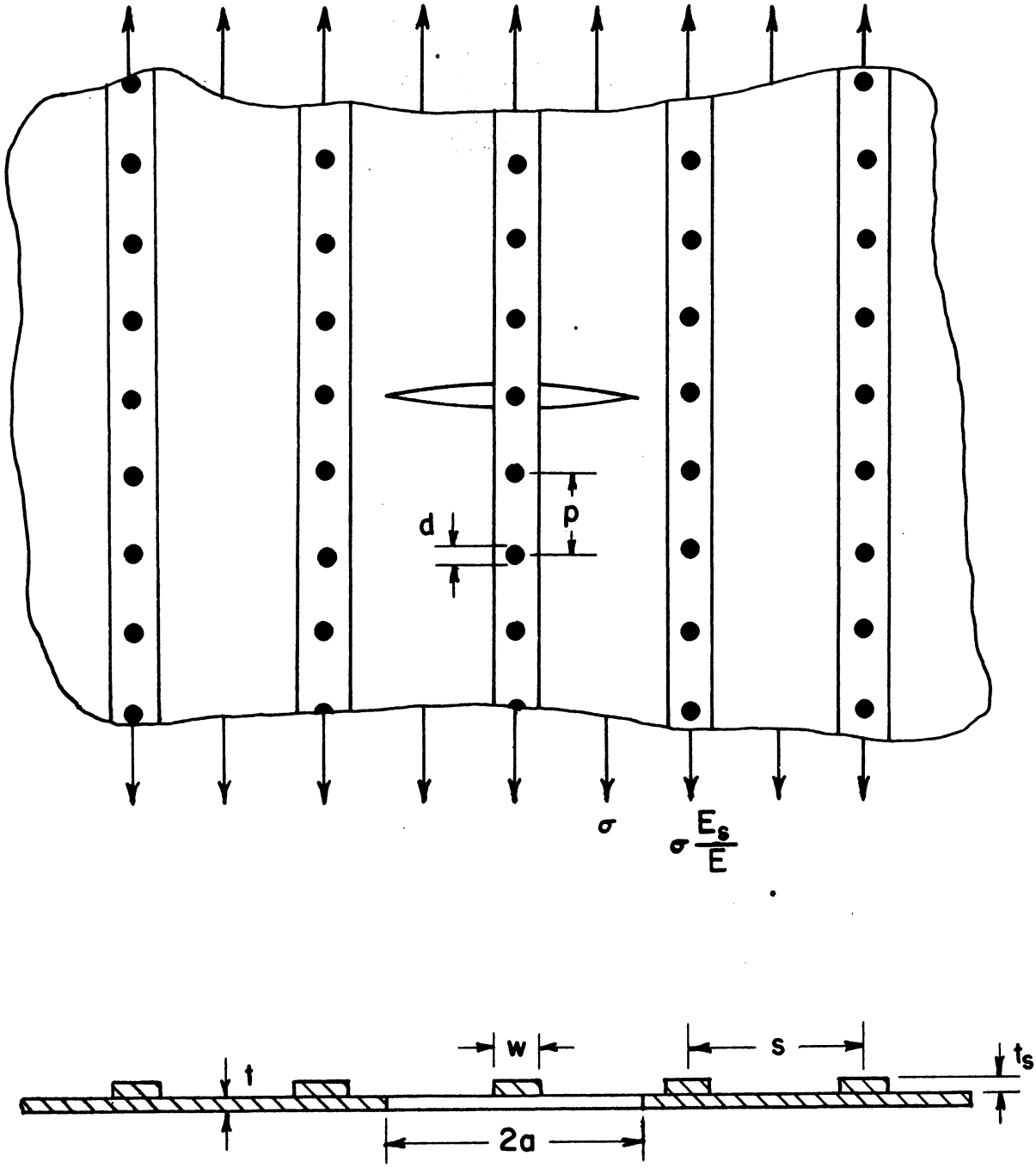

Figure 1.- Cracked sheet with riveted and uniformly spaced stringers.

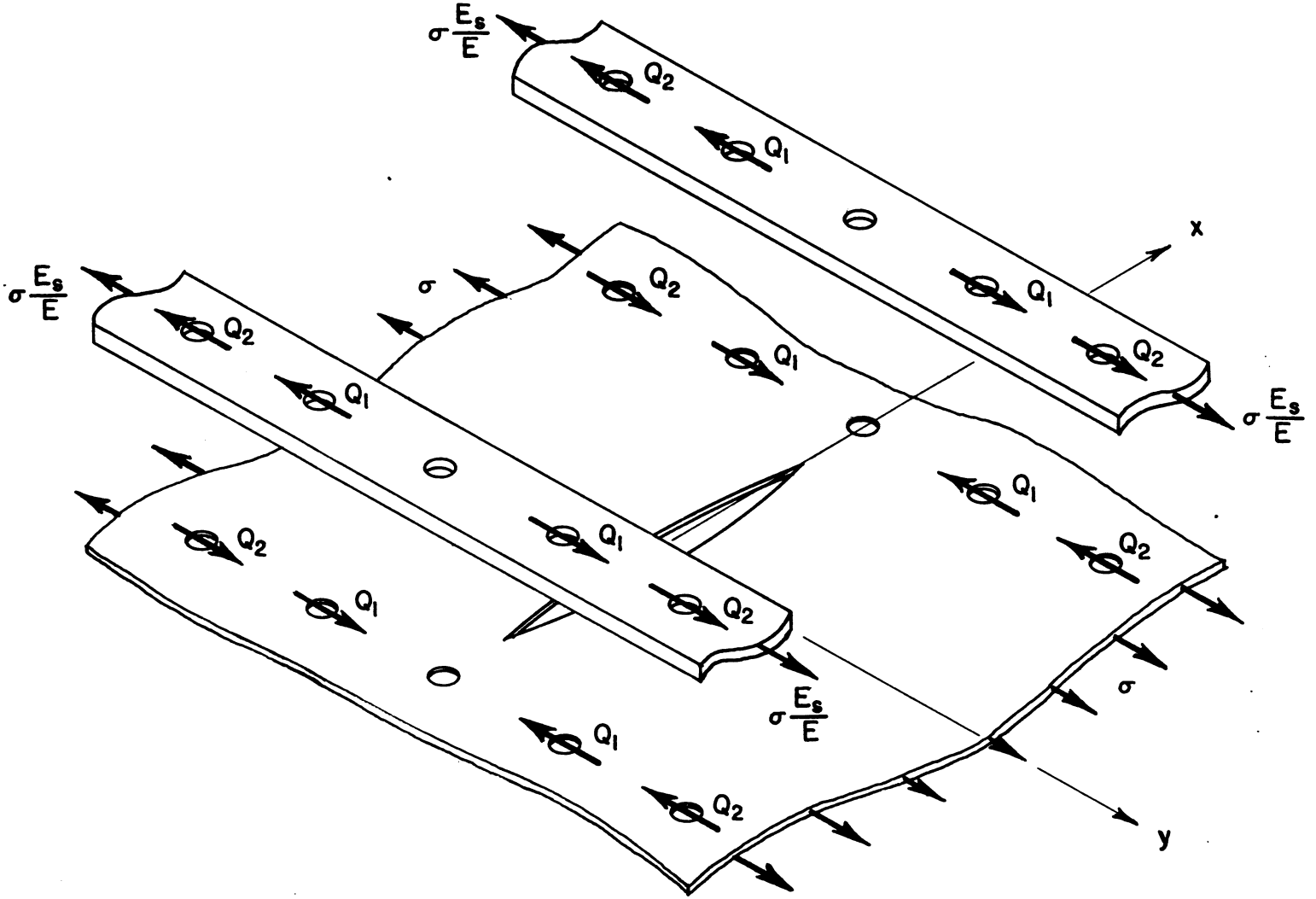

Figure 2.- Equilibrium of forces in cracked sheet and stringers.

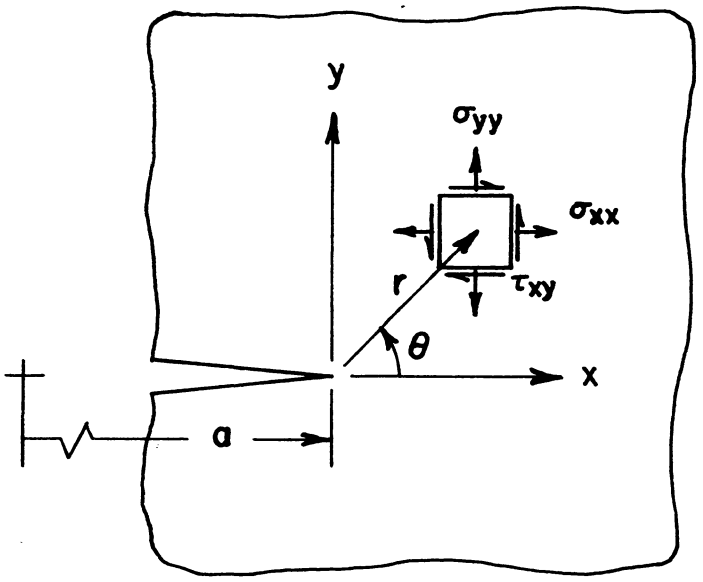

$$\sigma_{yy} = \frac{K}{\sqrt{2r}} \cos\frac{\theta}{2}\left[1 + \sin\frac{\theta}{2}\sin\frac{3\theta}{2}\right]$$

$$\sigma_{xx} = \frac{K}{\sqrt{2r}} \cos\frac{\theta}{2}\left[1 - \sin\frac{\theta}{2}\sin\frac{3\theta}{2}\right]$$

$$\tau_{xy} = \frac{K}{\sqrt{2r}} \sin\frac{\theta}{2}\cos\frac{\theta}{2}\cos\frac{3\theta}{2}$$

$$\tau_{xz} = \tau_{yz} = 0$$

Figure 3.- Coordinate system and equations relating the stress intensity factor to the elastic stresses in the vicinity of a crack tip - mode I.

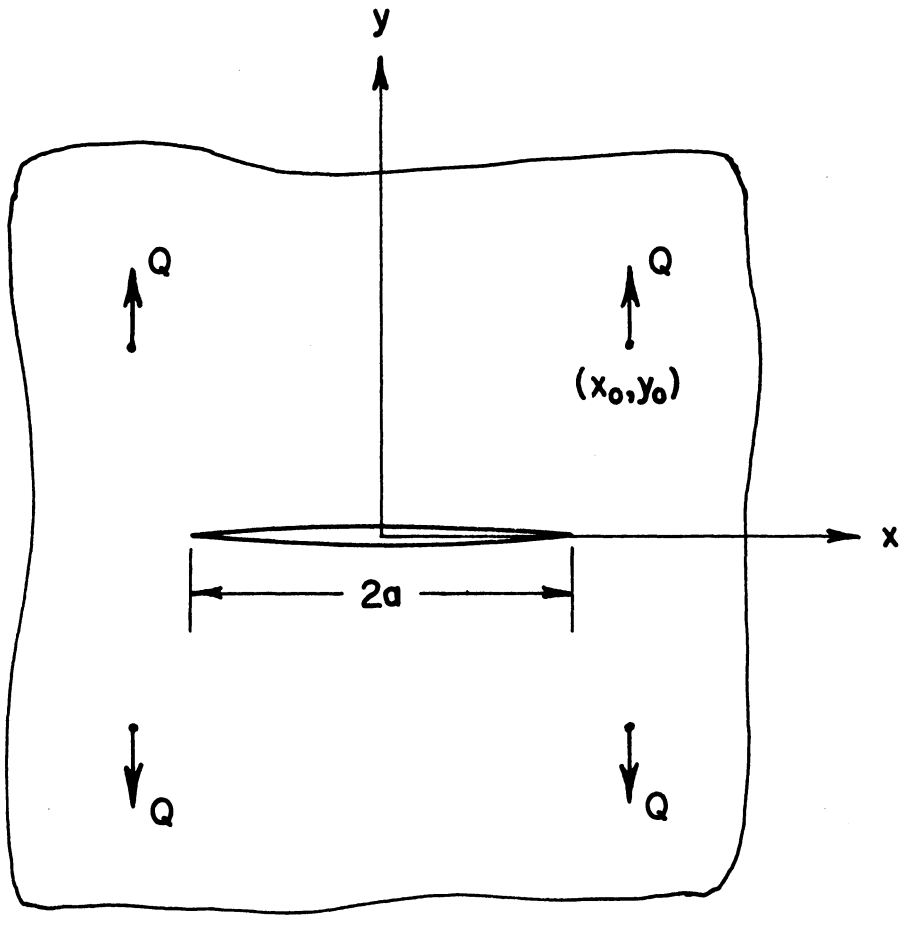

Figure 4.- Cracked sheet with symmetrically applied point forces.

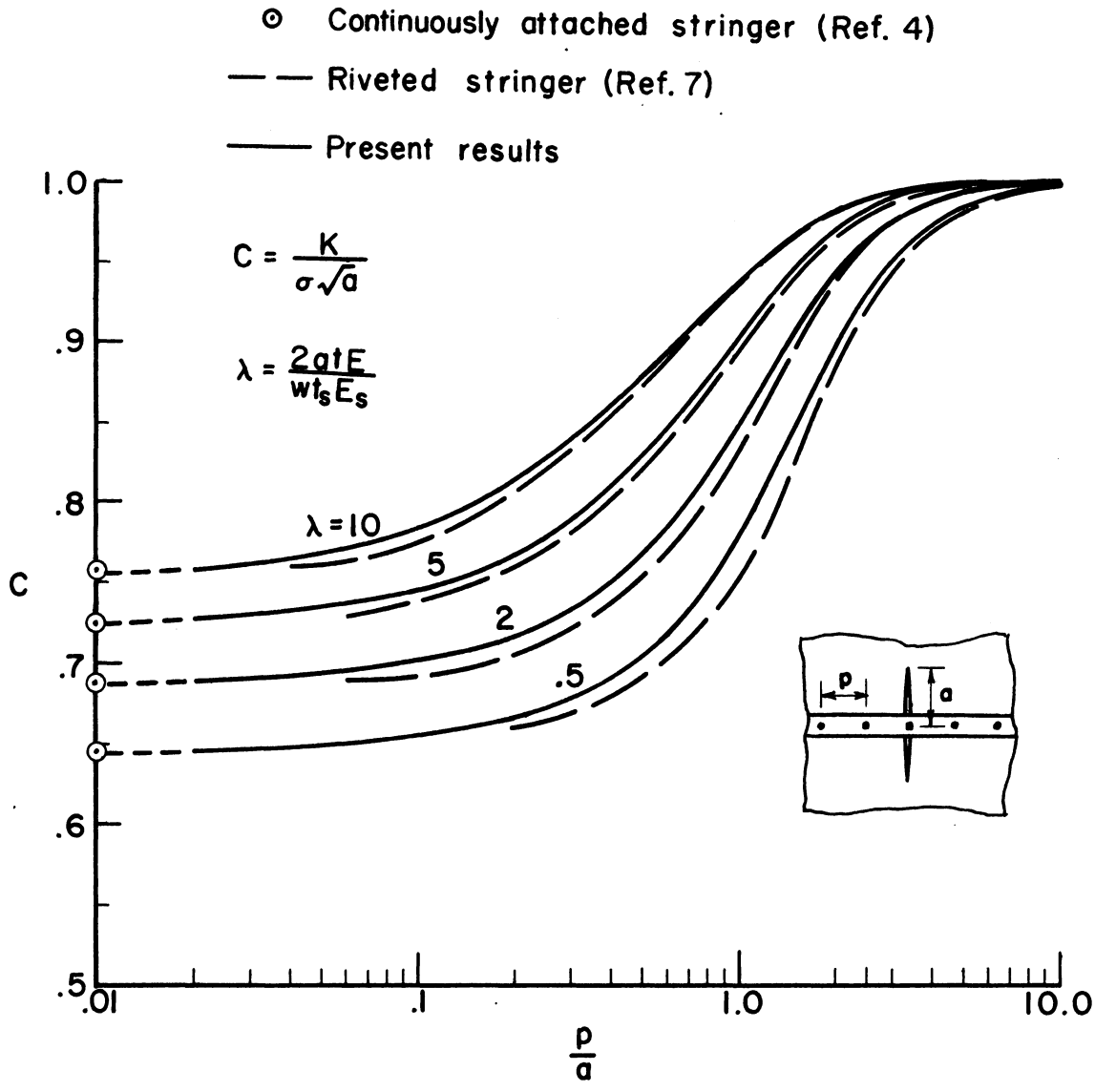

(a) Stress intensity correction factor.

Figure 5.- Comparison of results for the problem of a single stringer.

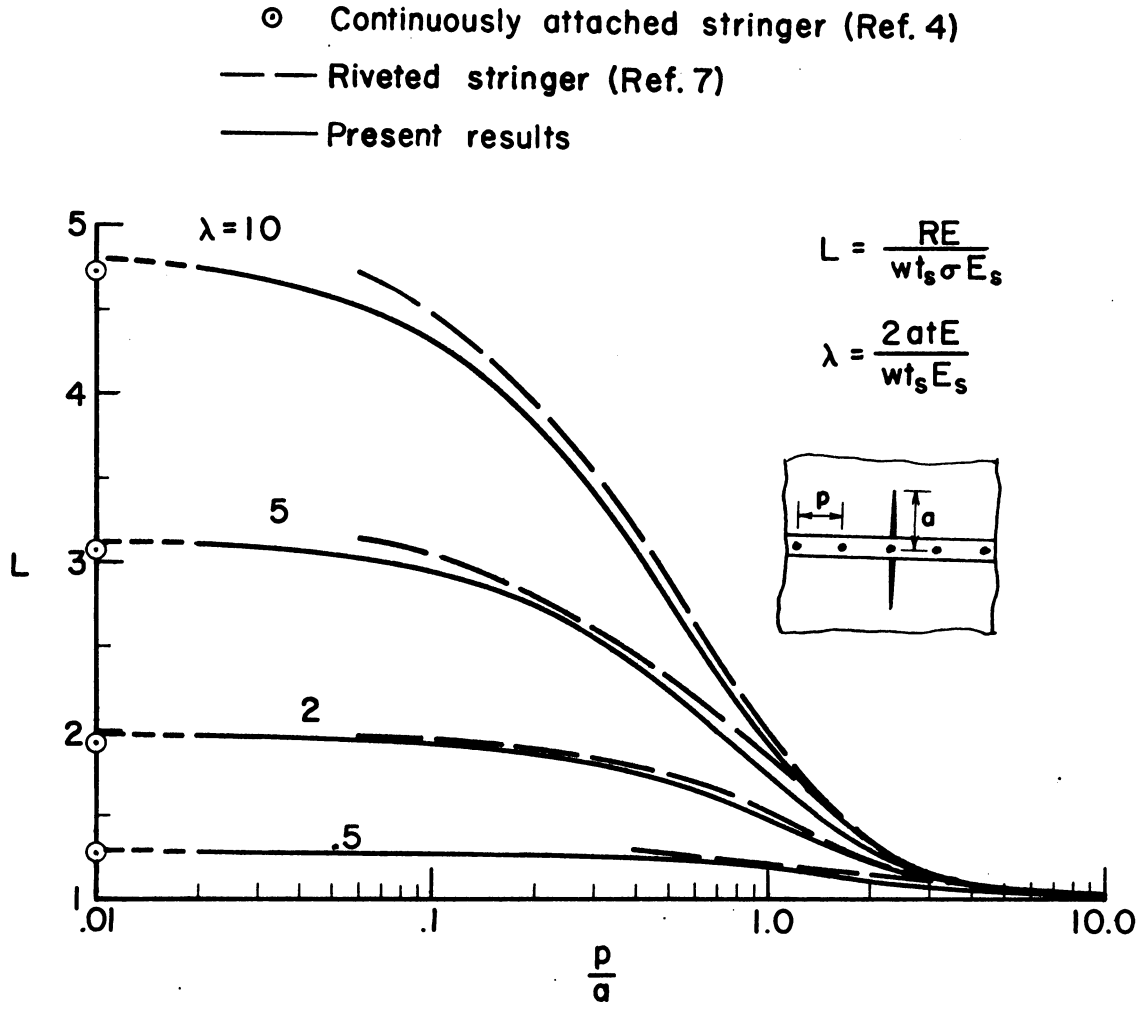

(b) Stringer load concentration factor.

Figure 5.- Concluded.

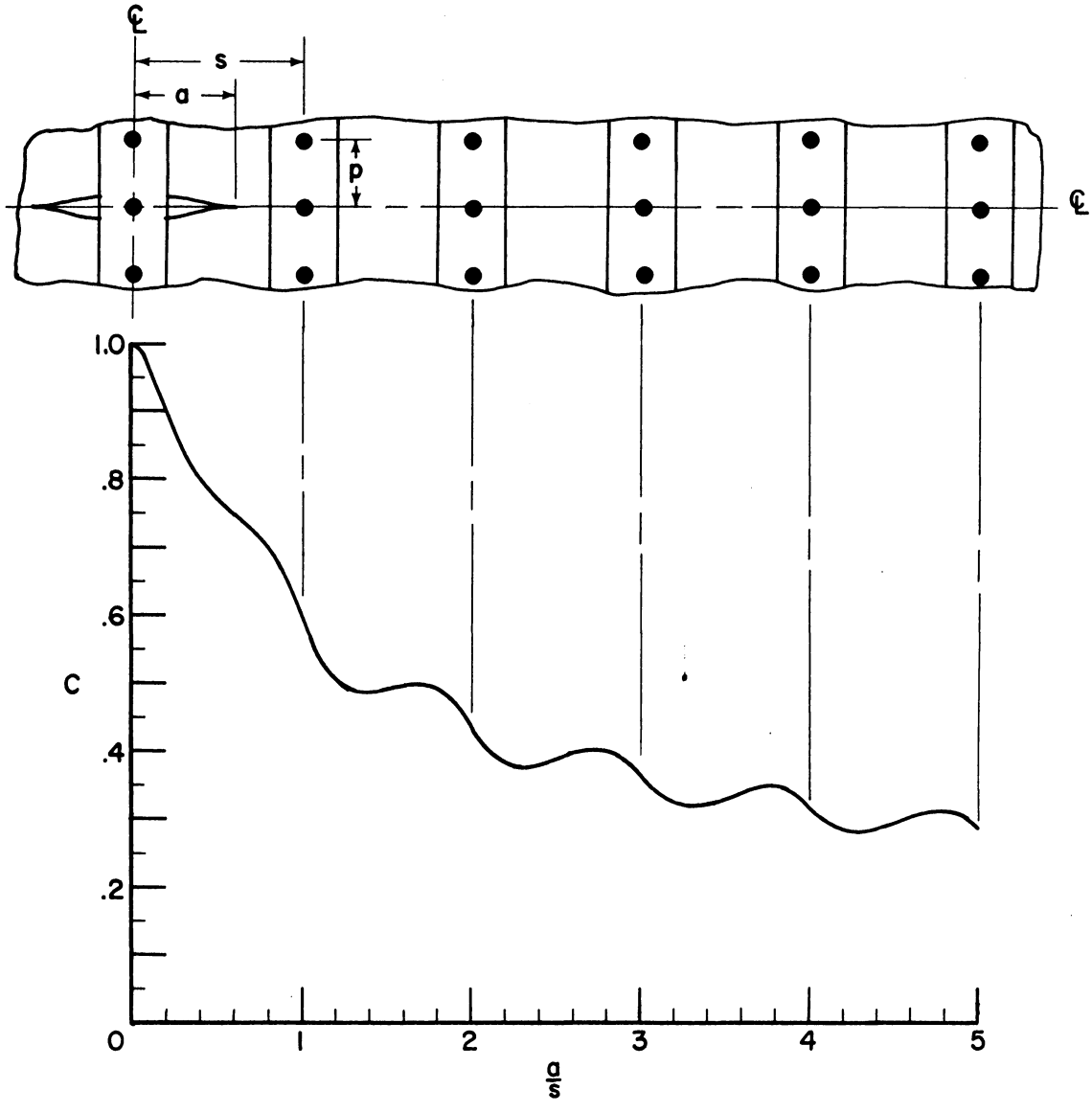

(a) Stress intensity correction factor.

Figure 6.- Typical results for the problem of riveted and uniformly spaced stringers. (50 percent stiffening, s/p = 2.5, p/d = 4, w/d = 5.)

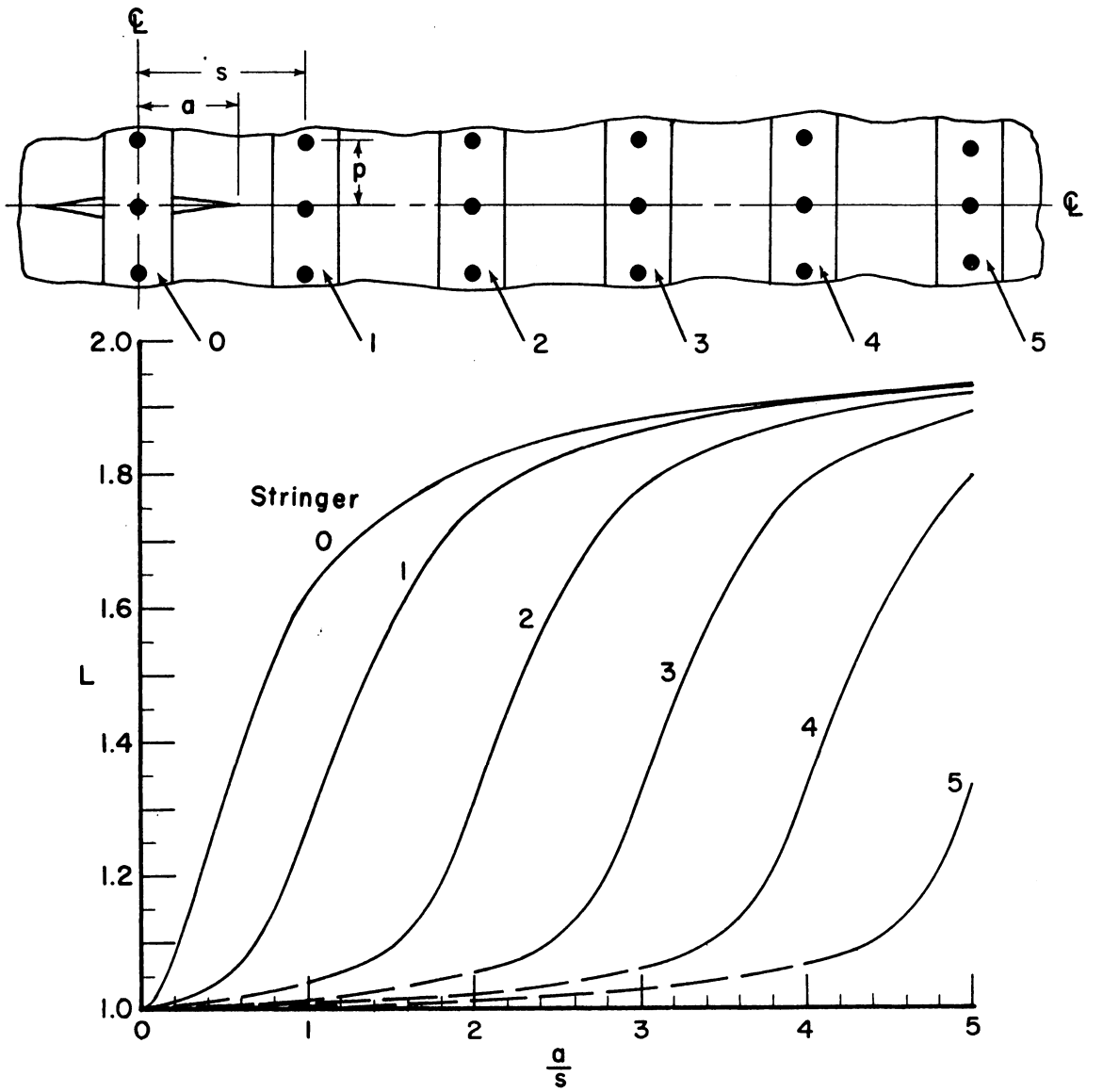

(b) Stringer load concentration factor.

Figure 6.- Continued.

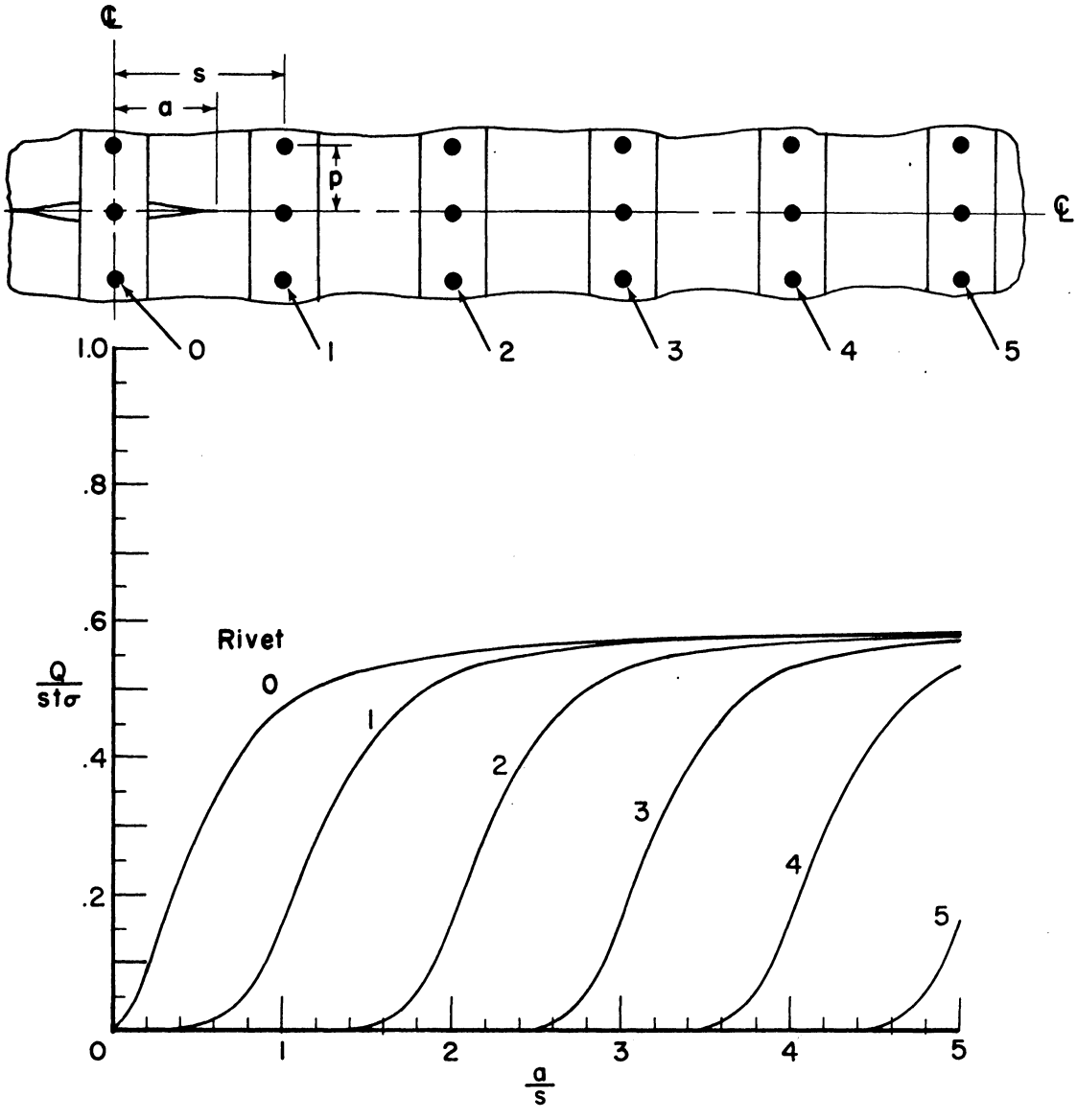

(c) Rivet forces in stringer at crack origin.

Figure 6.- Continued.

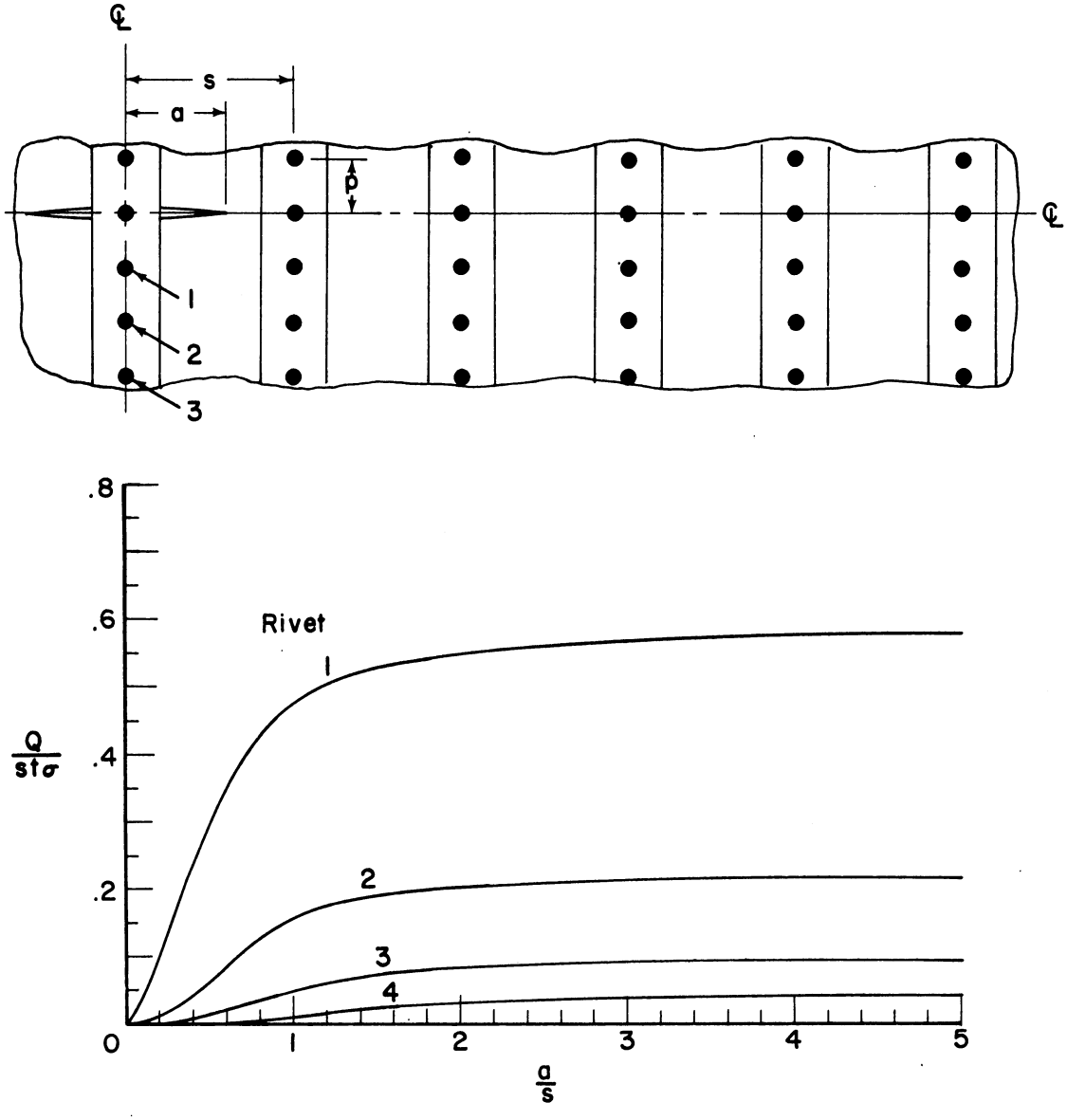

(d) Force in first rivet of each stringer.

Figure 6.- Concluded.

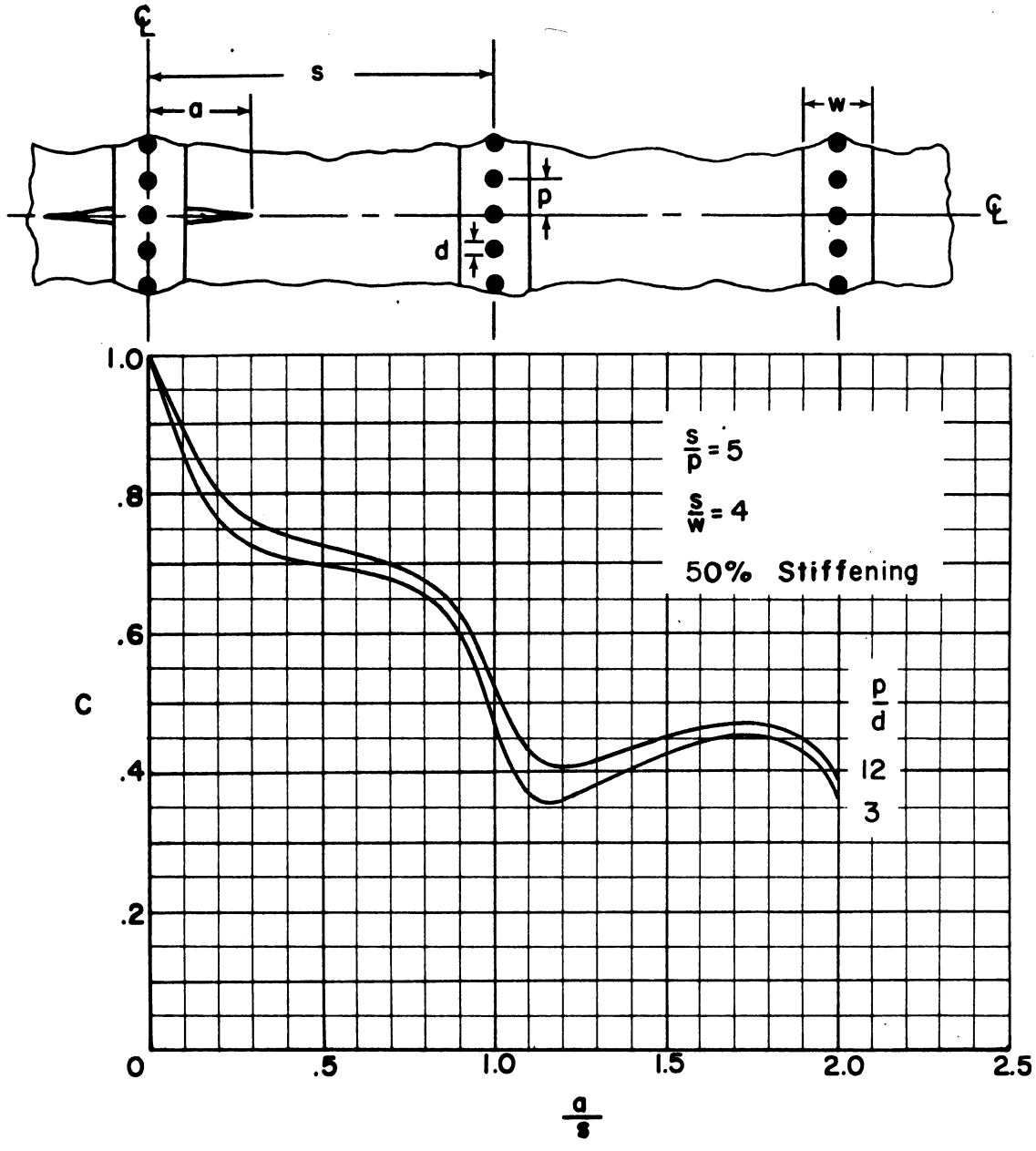

Figure 7.- Effect of rivet diameter on the stress intensity correction factor.

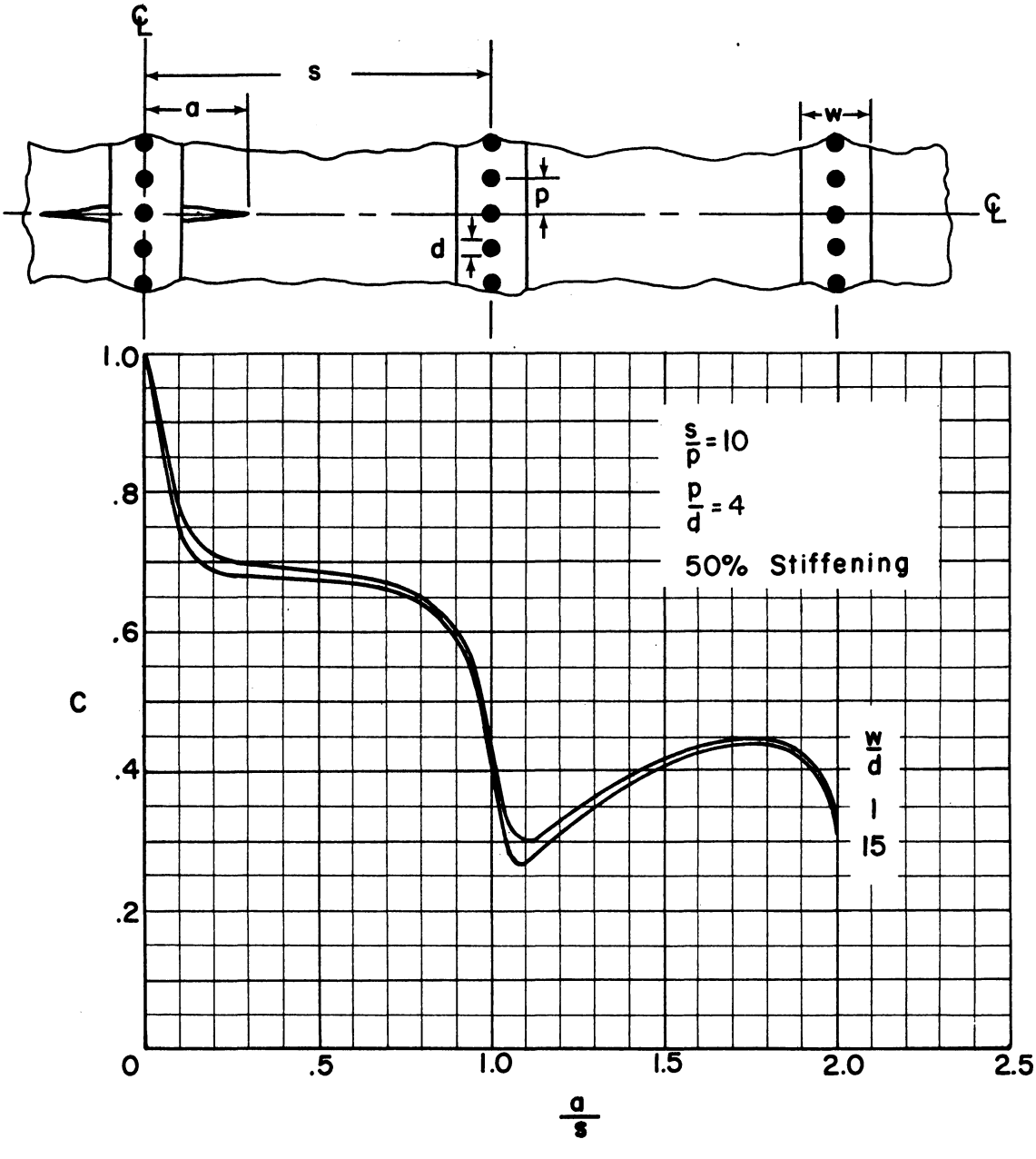

Figure 8.- Effect of stringer shape on the stress intensity correction factor.

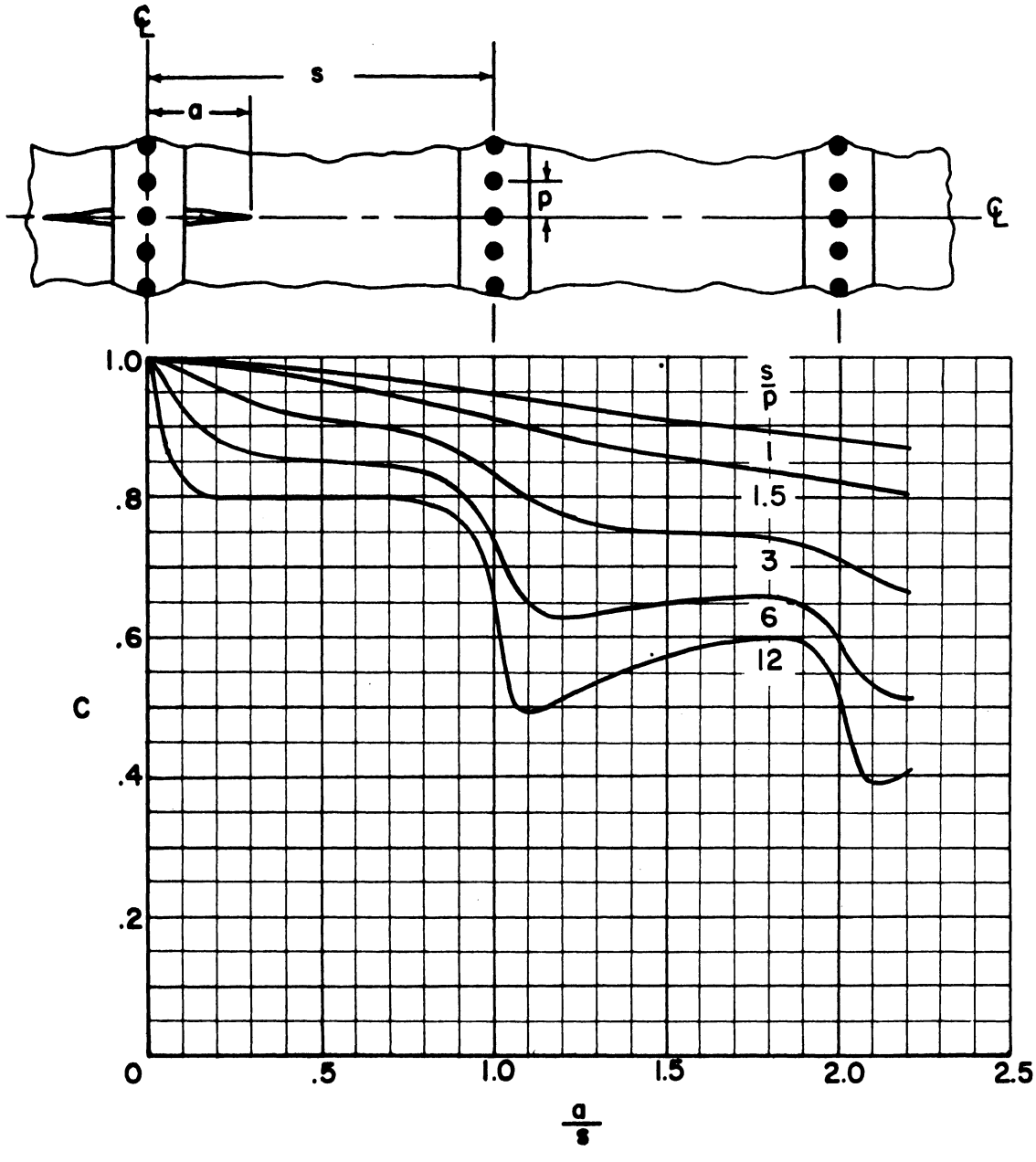

(a) 10 percent stiffening.

Figure 9.- Effect of crack length and rivet and stringer spacing on the stress intensity correction factor. Crack initiating at a rivet.

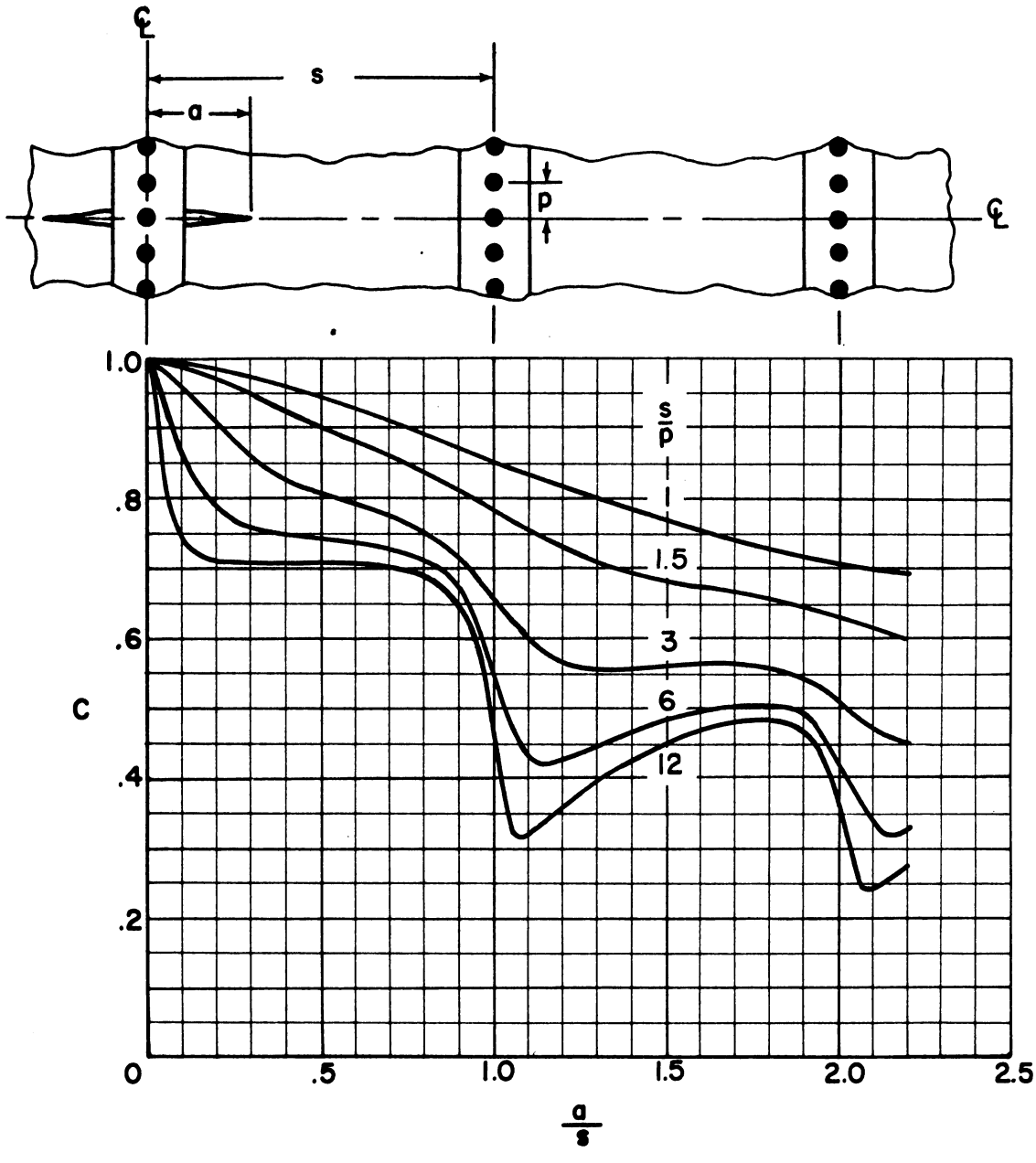

(b) 30 percent stiffening.

Figure 9.- Continued.

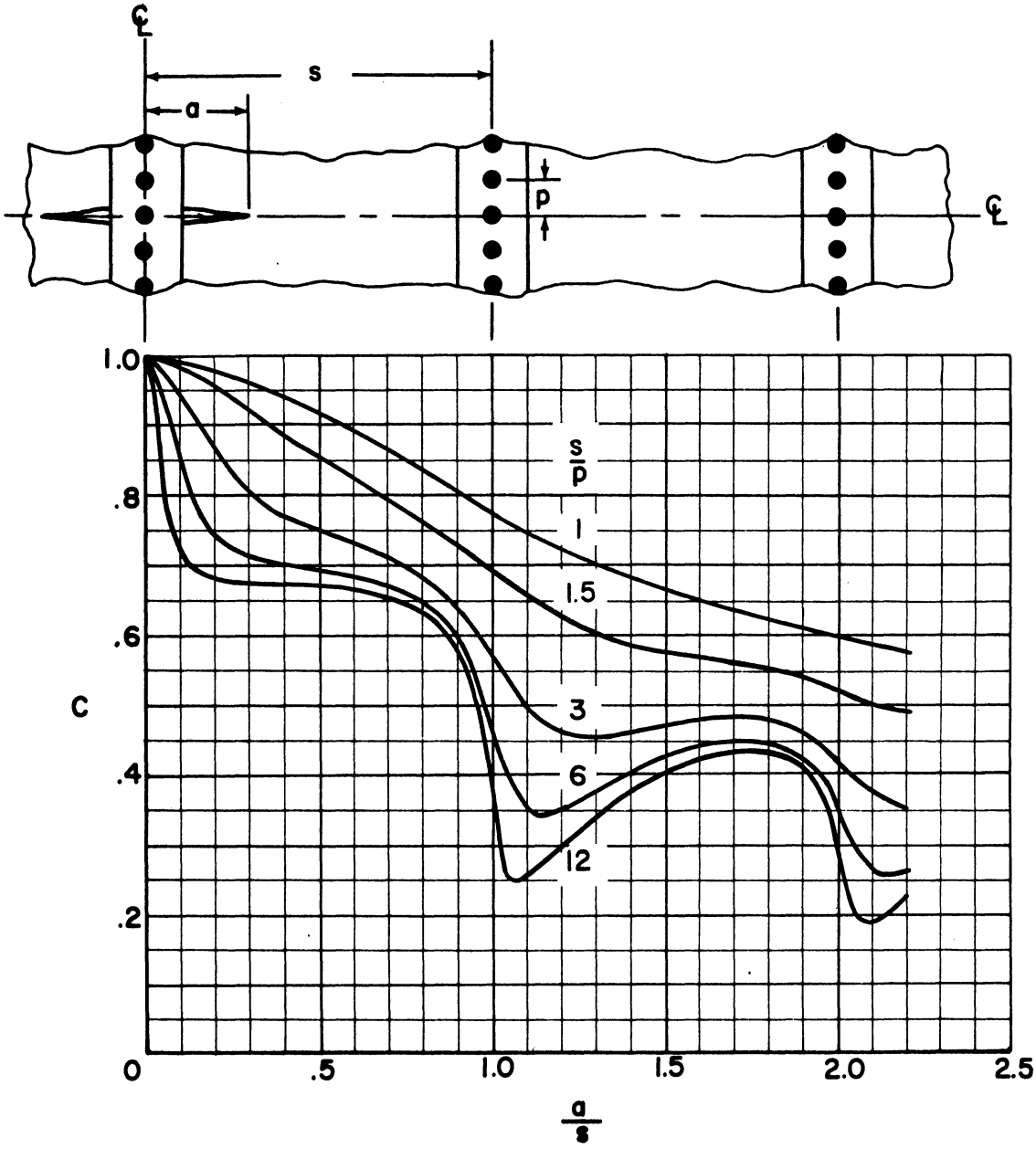

(c) 50 percent stiffening

Figure 9.- Continued.

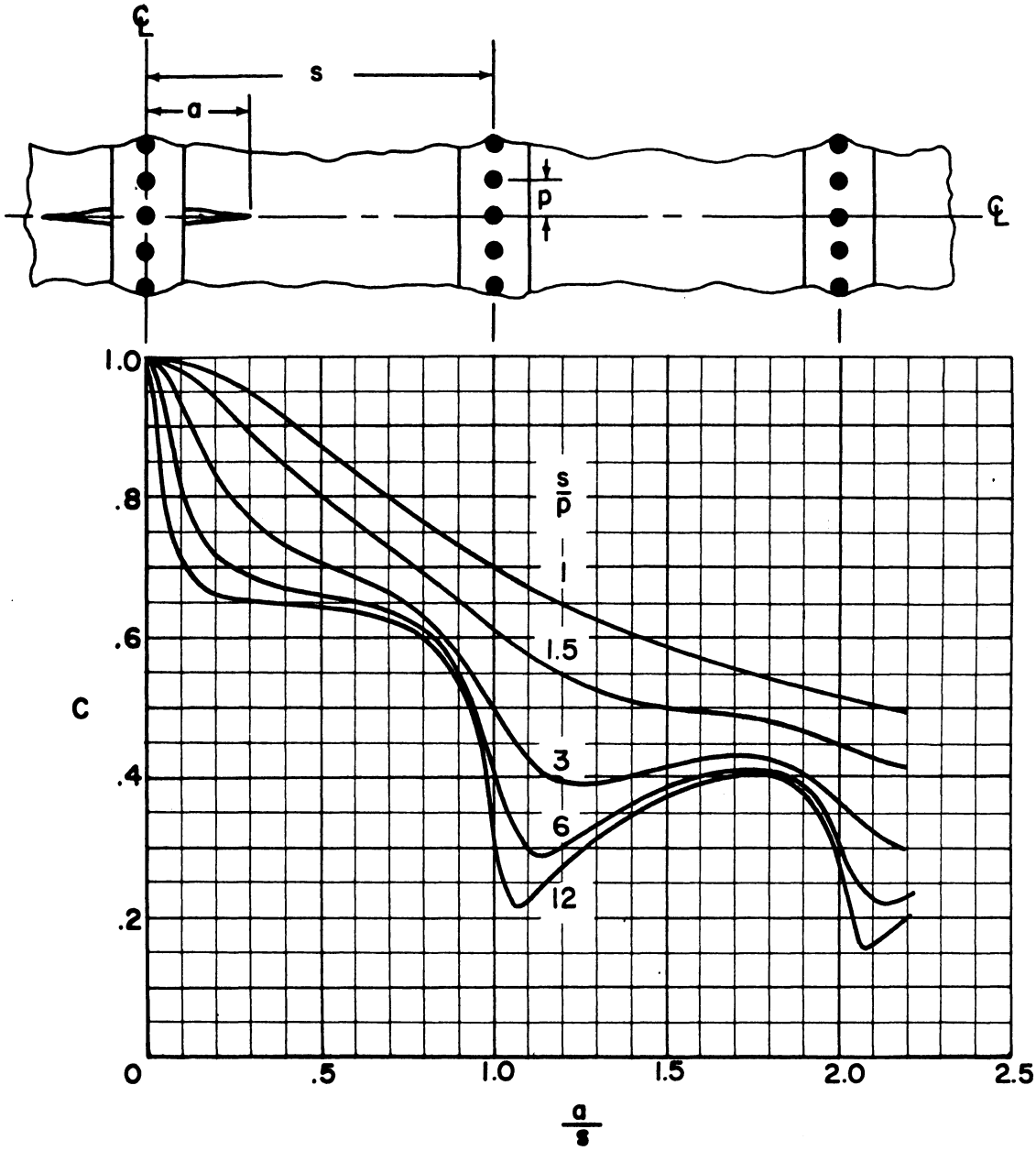

(d) 70 percent stiffening.

Figure 9.- Continued.

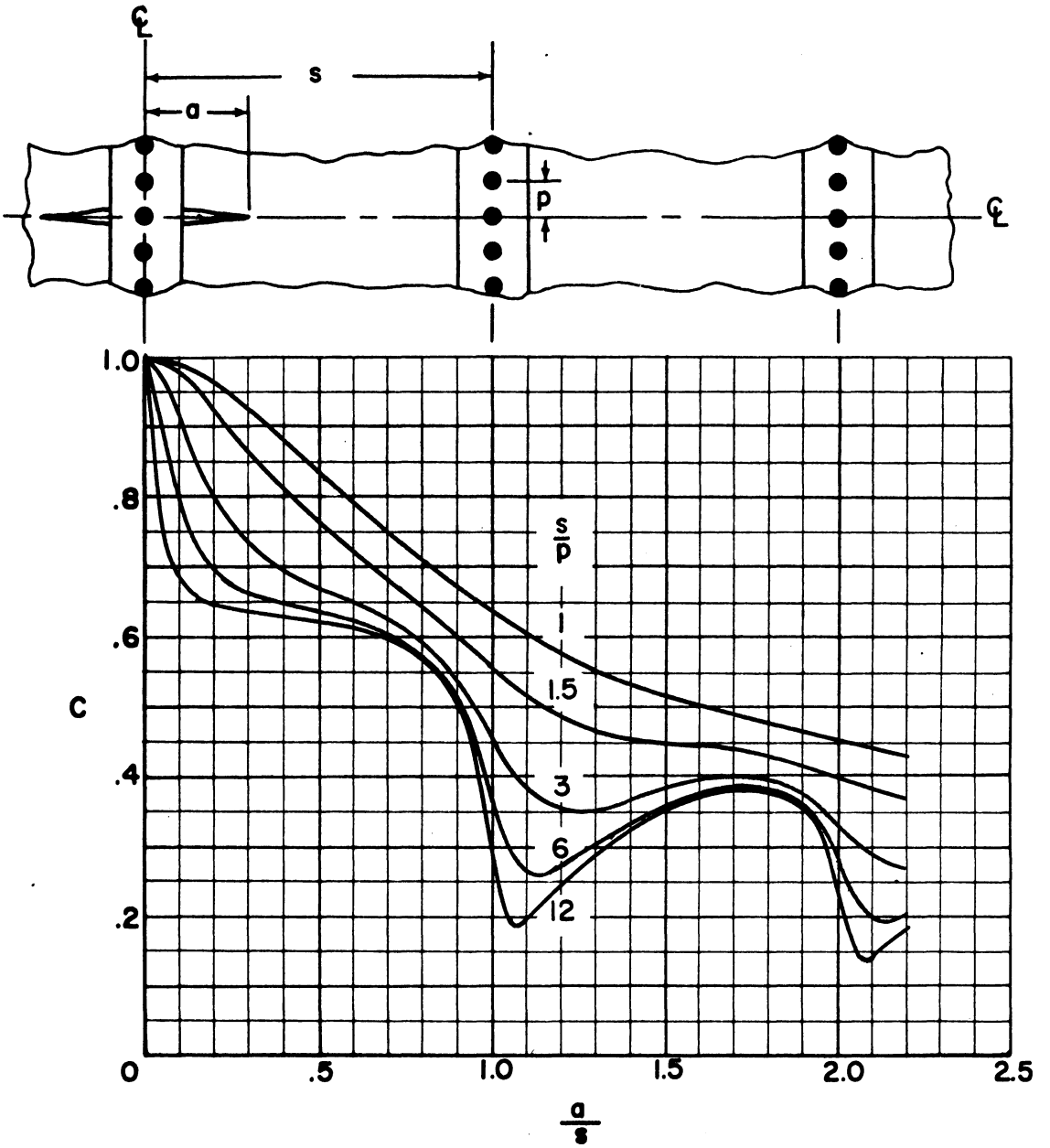

(e) 90 percent stiffening.

Figure 9.- Concluded.

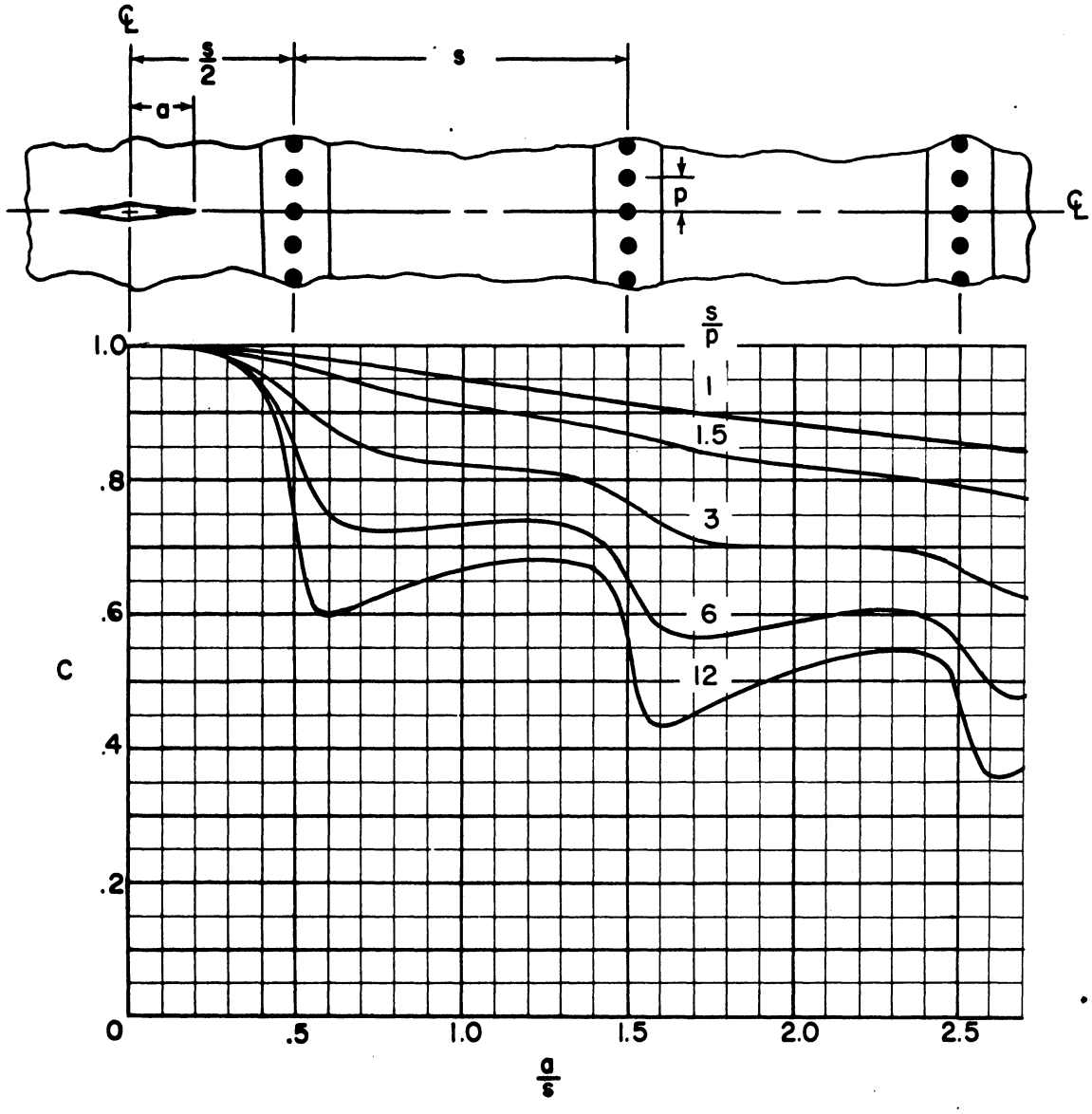

(a) 10 percent stiffening.

Figure 10.- Effect of crack length and rivet and stringer spacing on the stress intensity correction factor. Crack initiating between stringers.

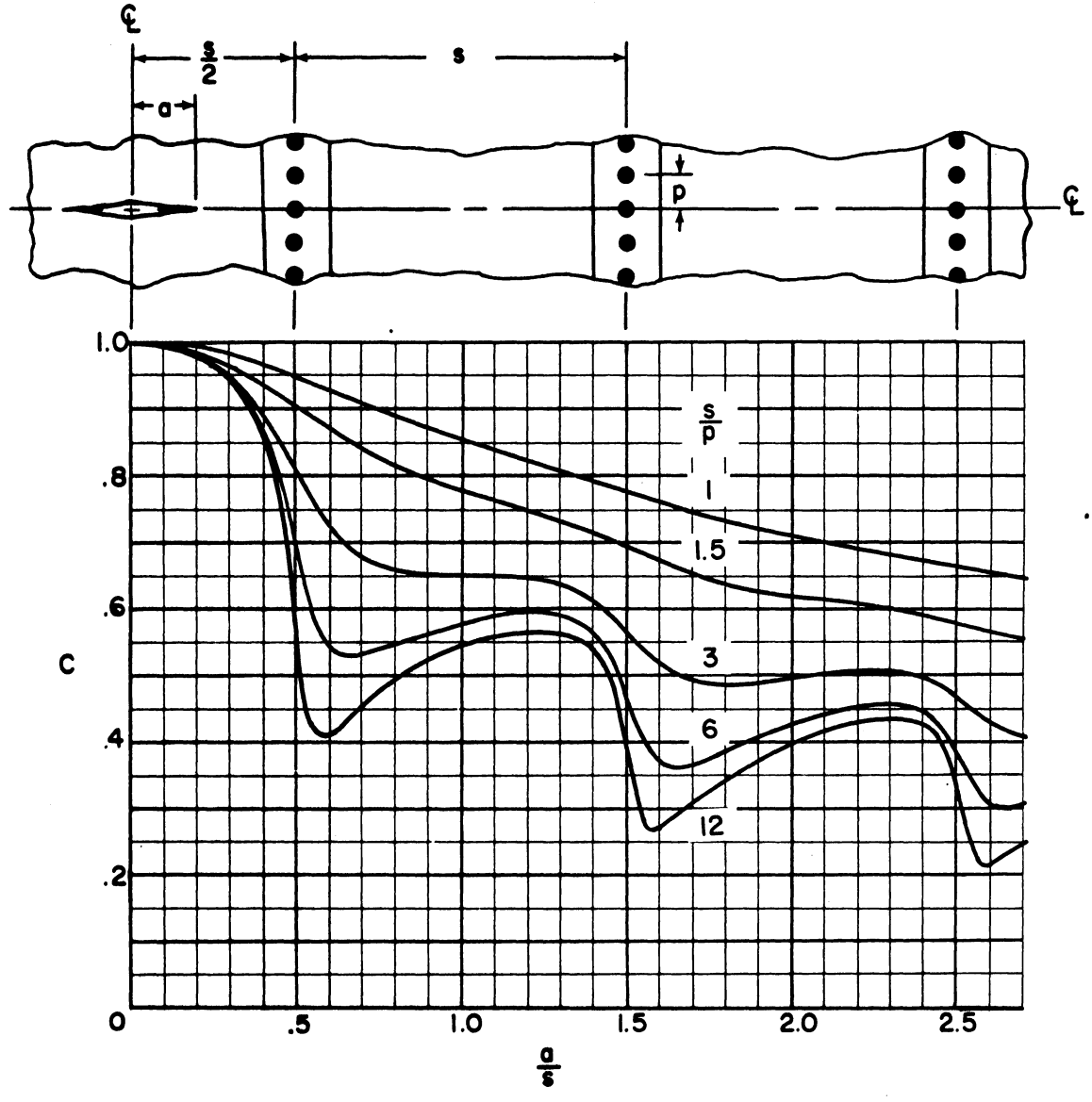

(b) 30 percent stiffening.

Figure 10.- Continued.

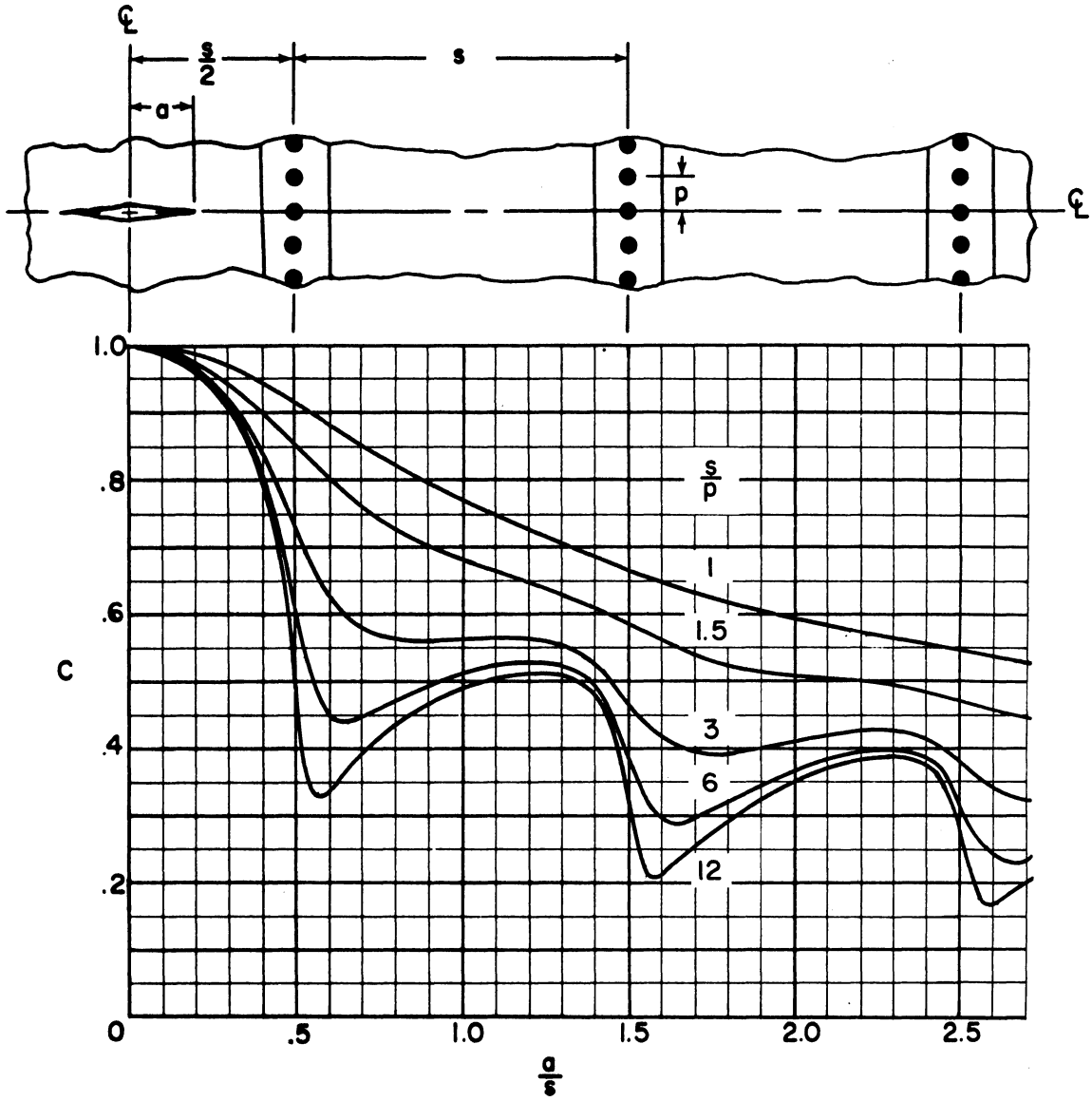

(c) 50 percent stiffening.

Figure 10.- Continued.

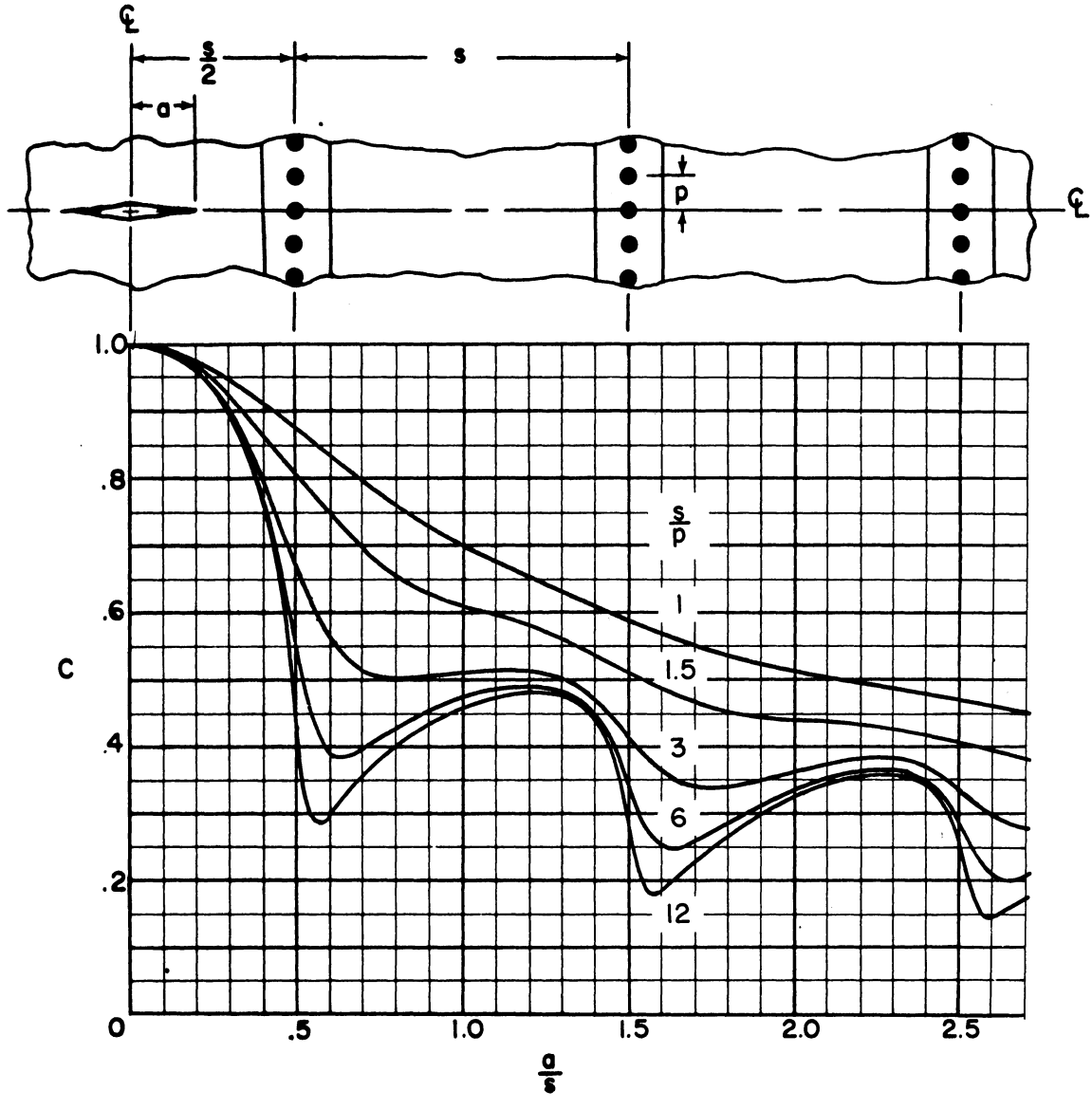

(d) 70 percent stiffening.

Figure 10.- Continued.

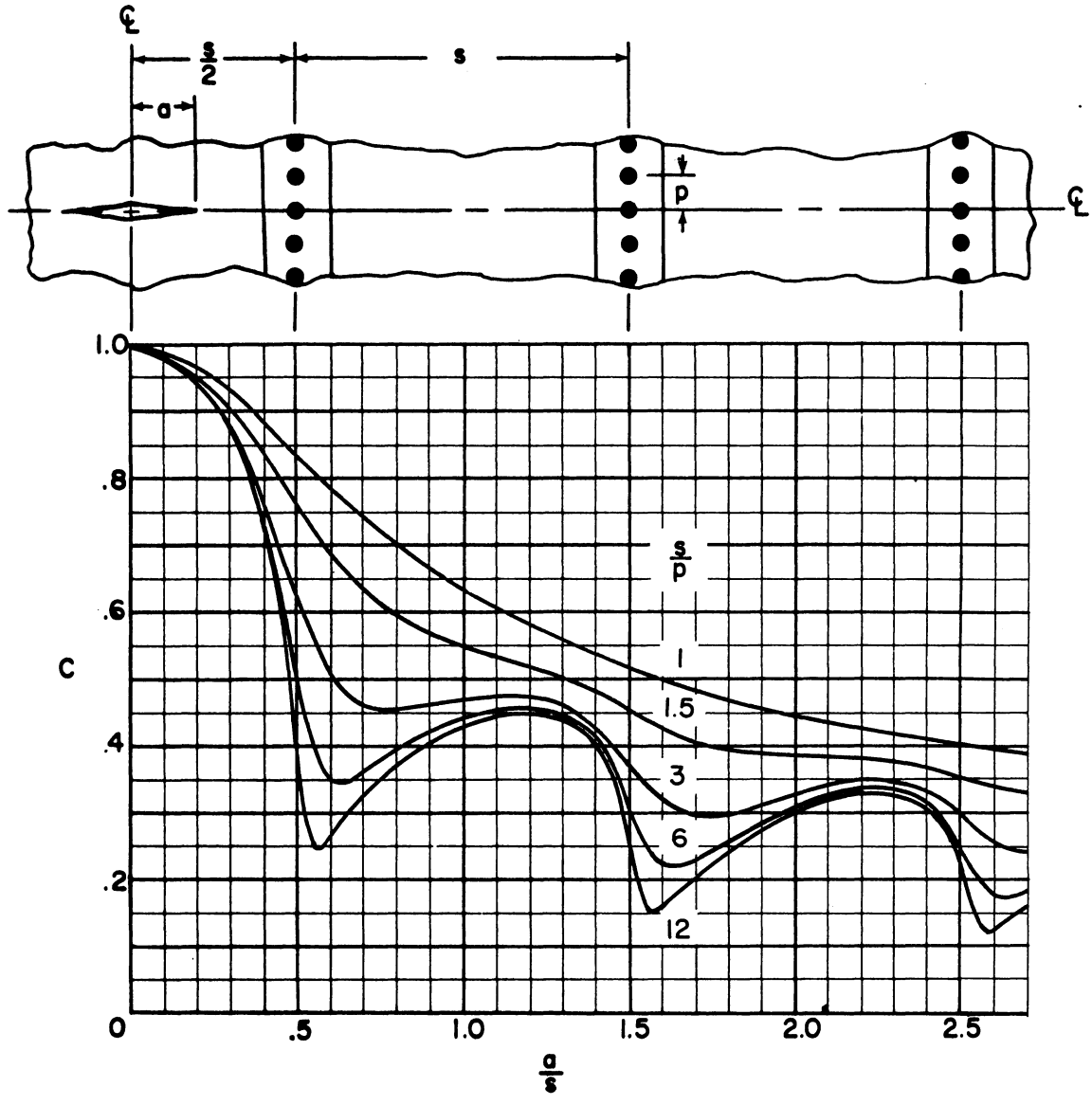

(e) 90 percent stiffening.

Figure 10.- Concluded.

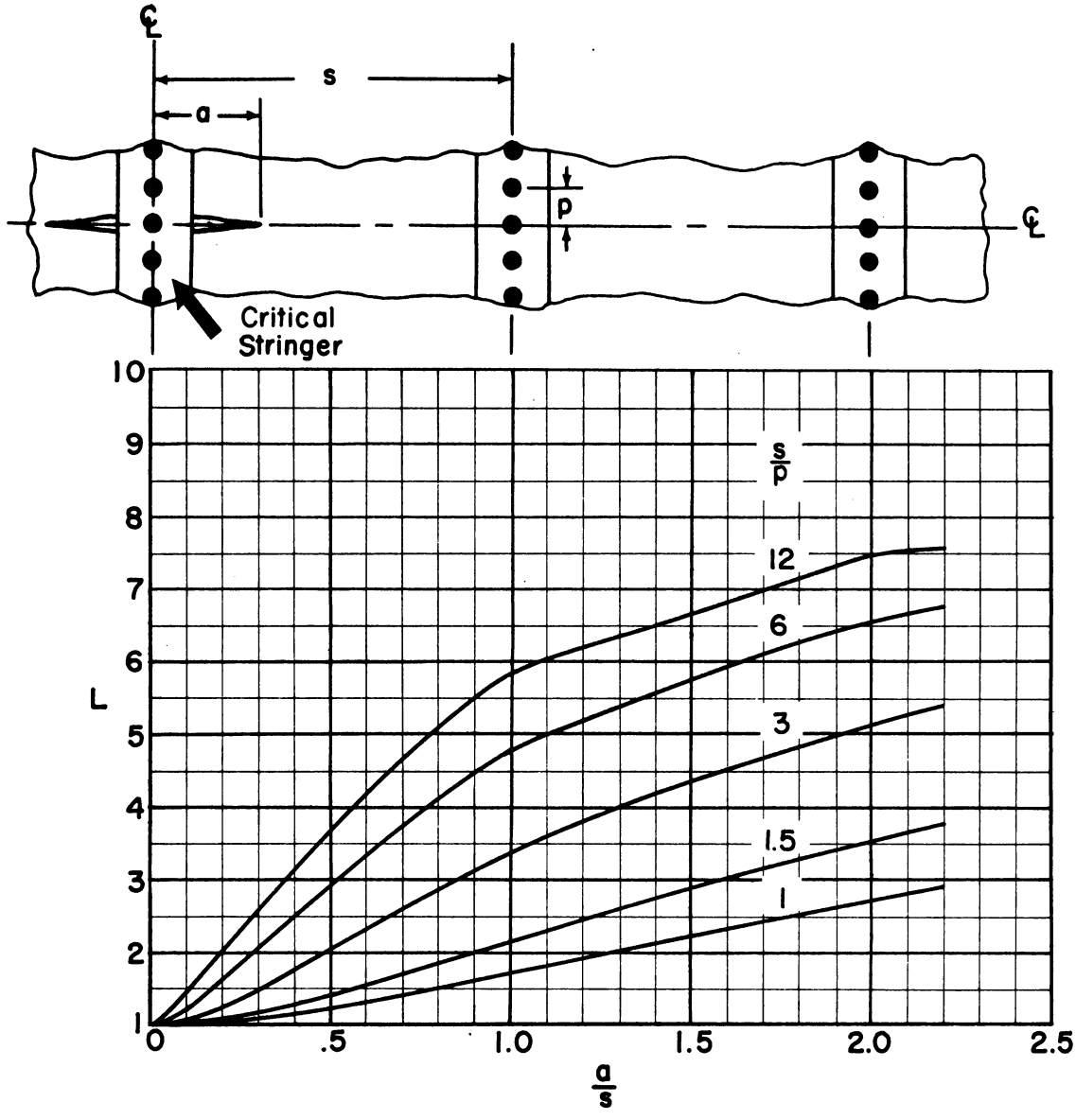

(a) 10 percent stiffening.

Figure 11.- Effect of crack length and rivet and stringer spacing on the stringer load concentration factor for the critical stringer. Crack initiating at a rivet.

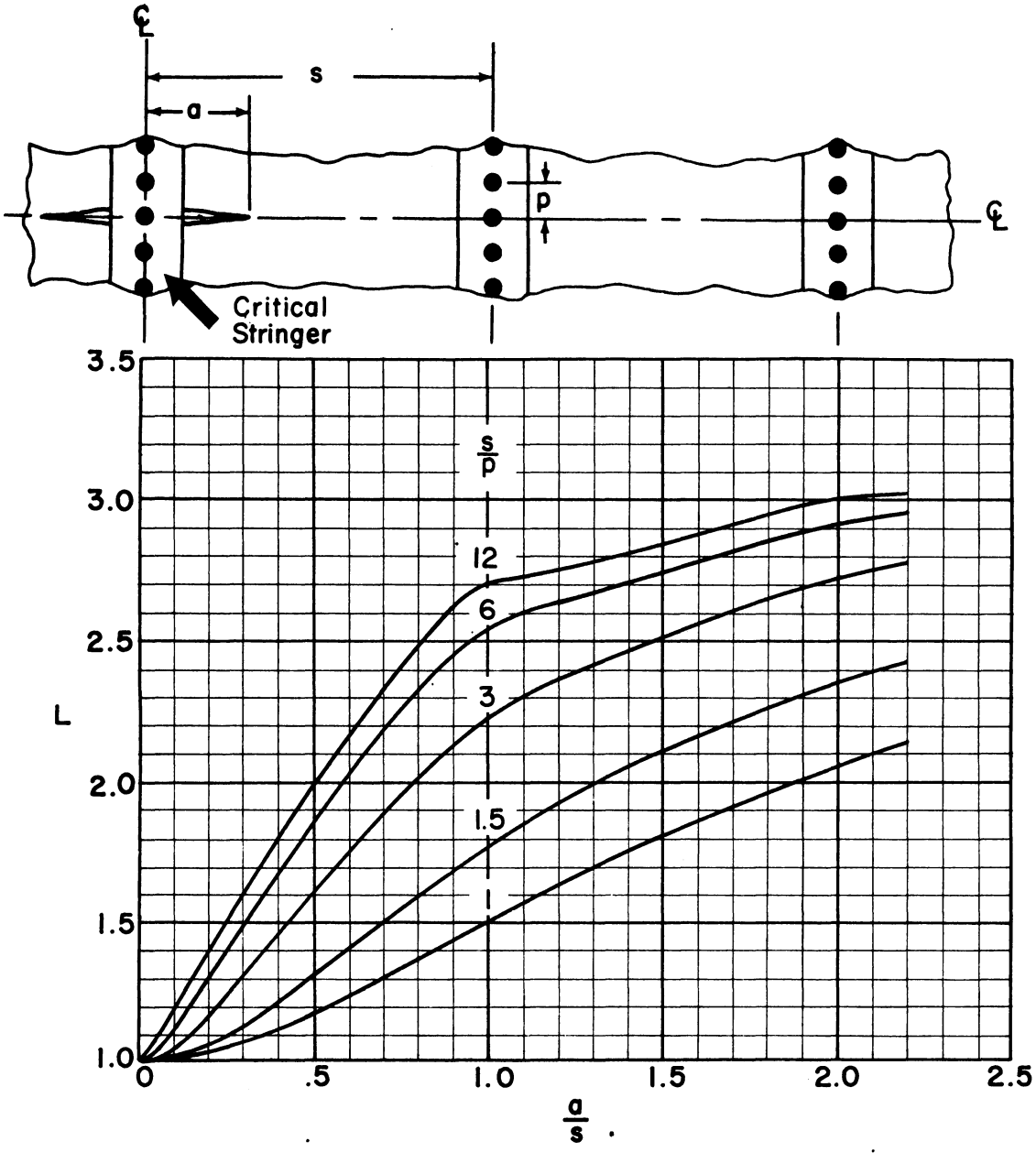

(b) 30 percent stiffening.

Figure 11.- Continued.

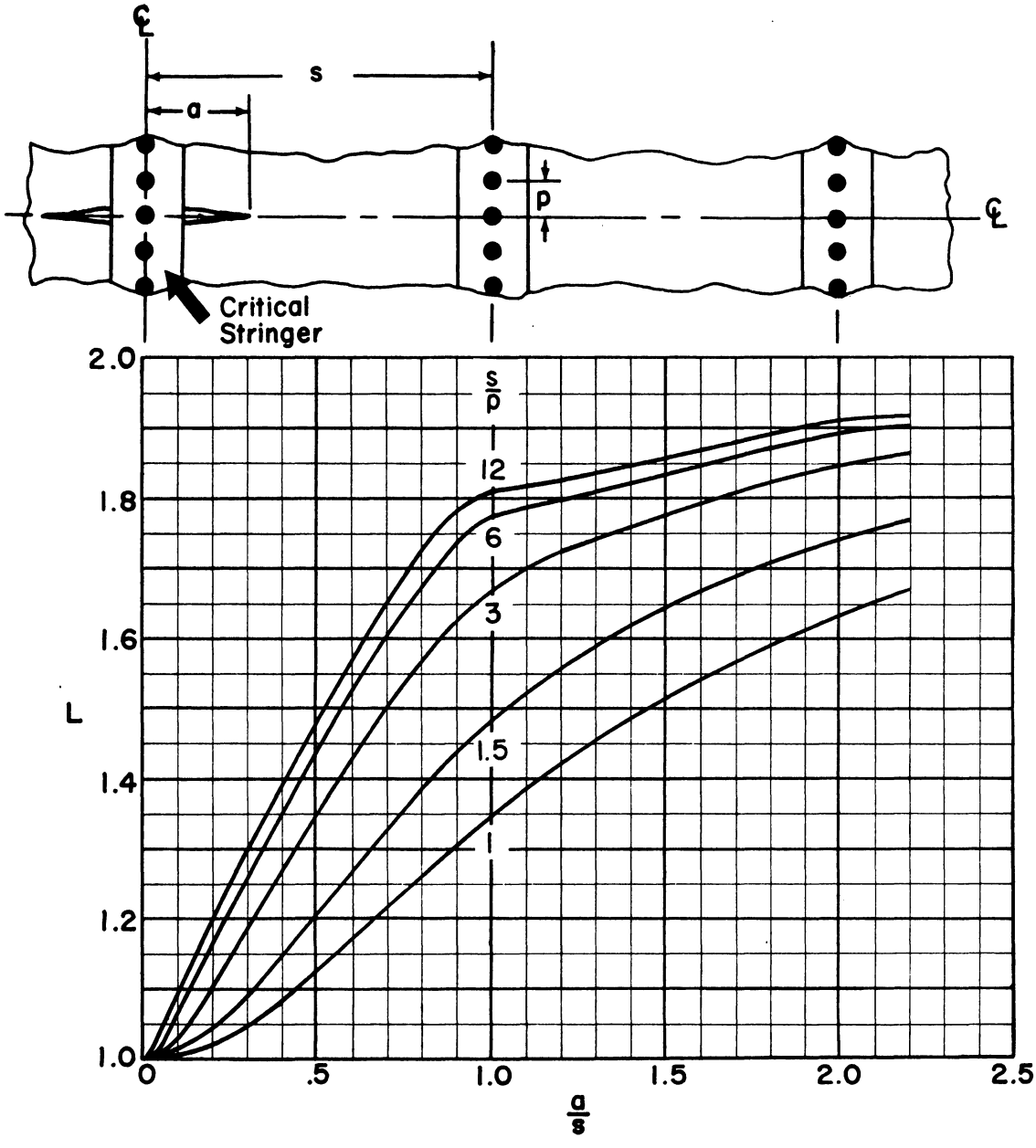

(c) 50 percent stiffening.

Figure 11.- Continued.

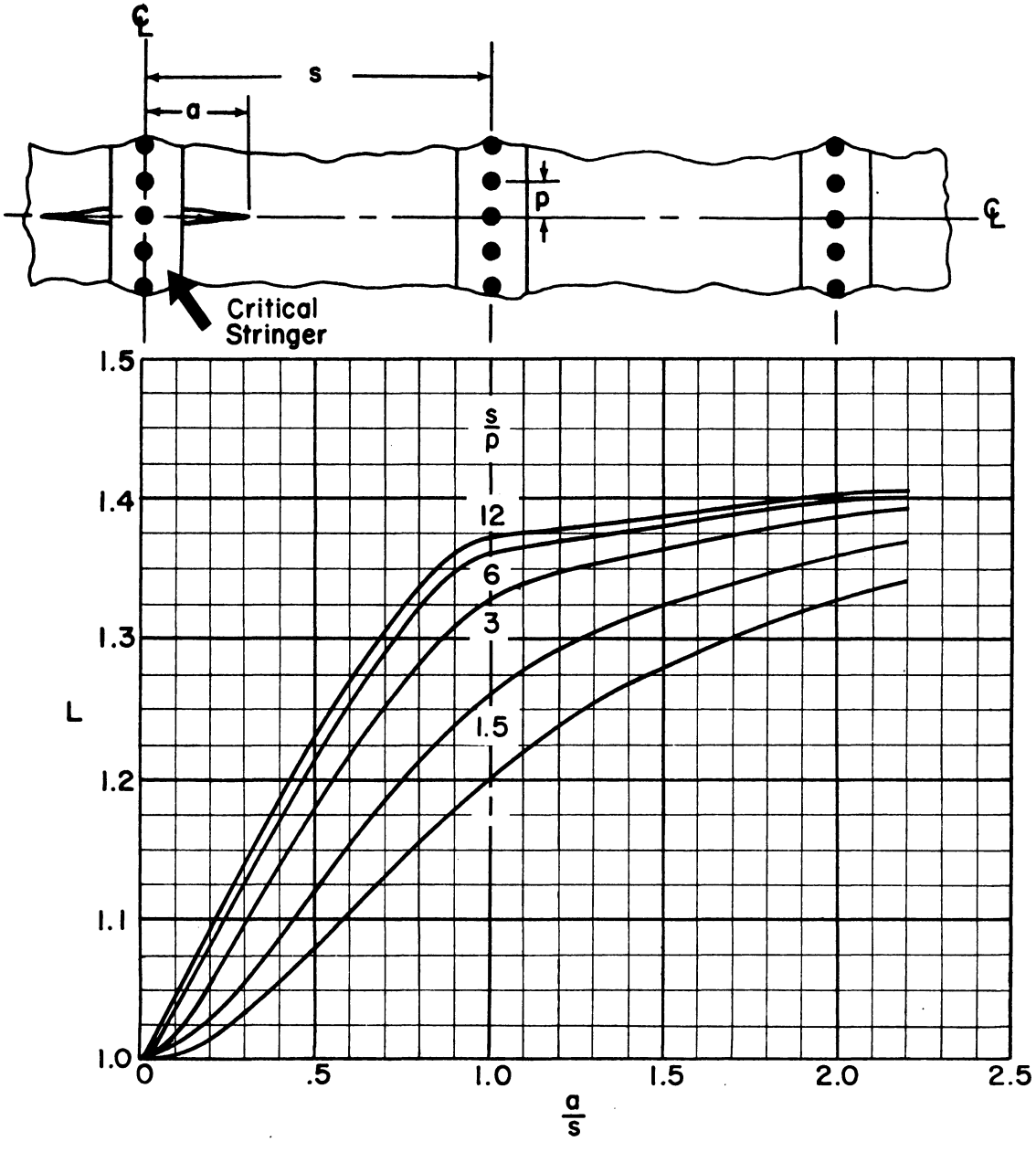

(d) 70 percent stiffening.

Figure 11.- Continued.

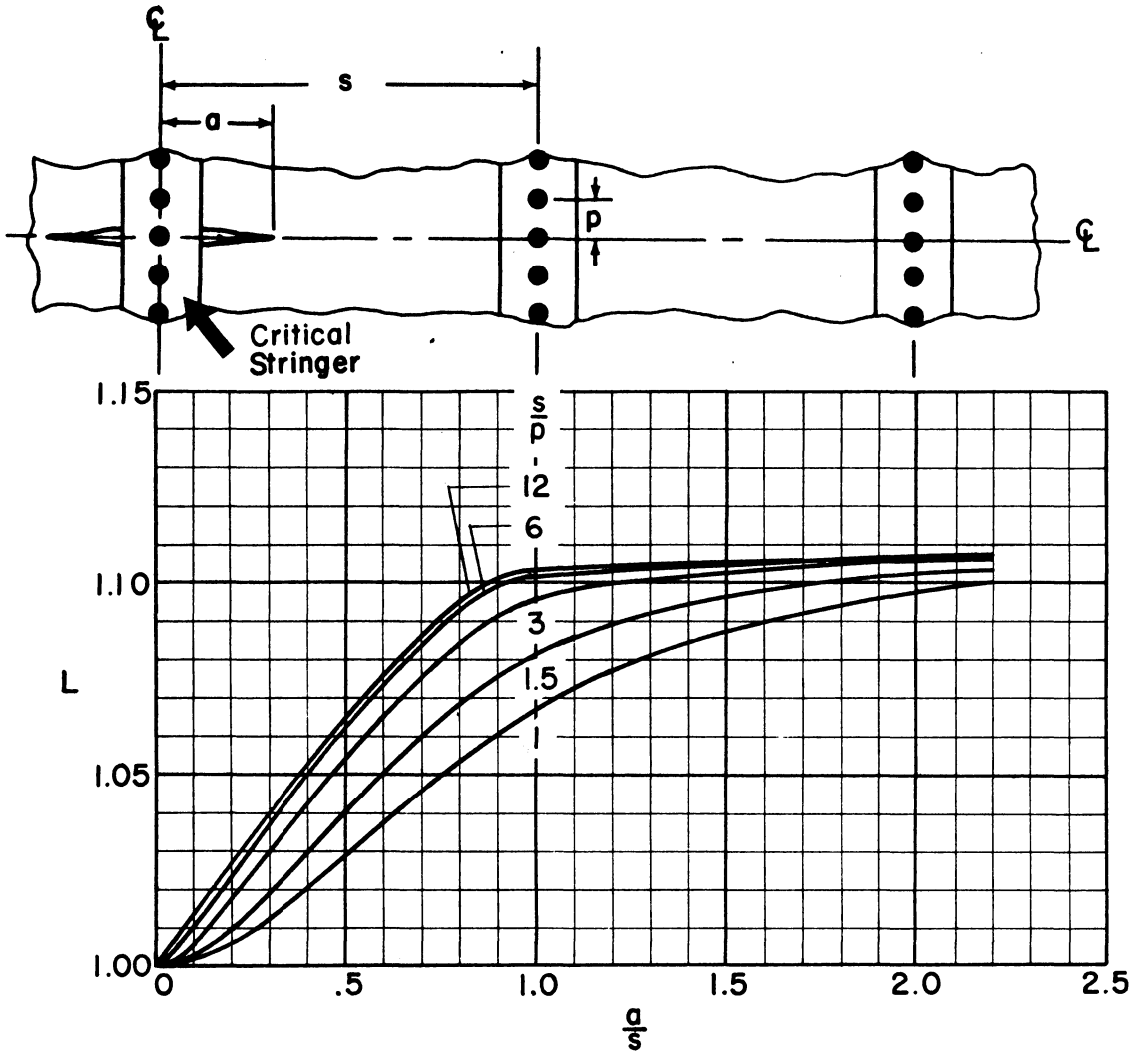

(e) 90 percent stiffening.

Figure 11.- Concluded.

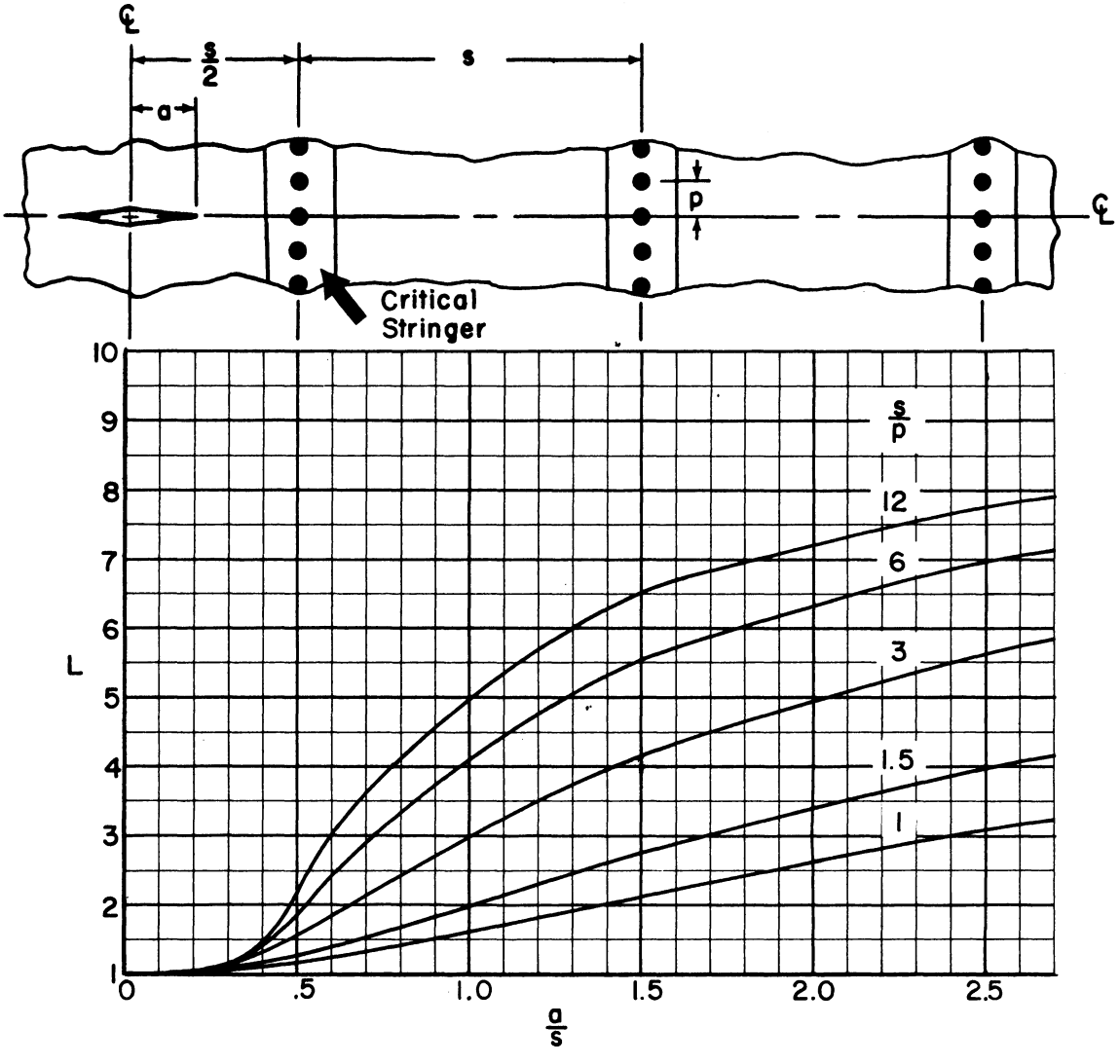

(a) 10 percent stiffening.

Figure 12.- Effect of crack length and rivet and stringer spacing on the stringer load concentration factor in the critical stringer. Crack initiating between stringers.

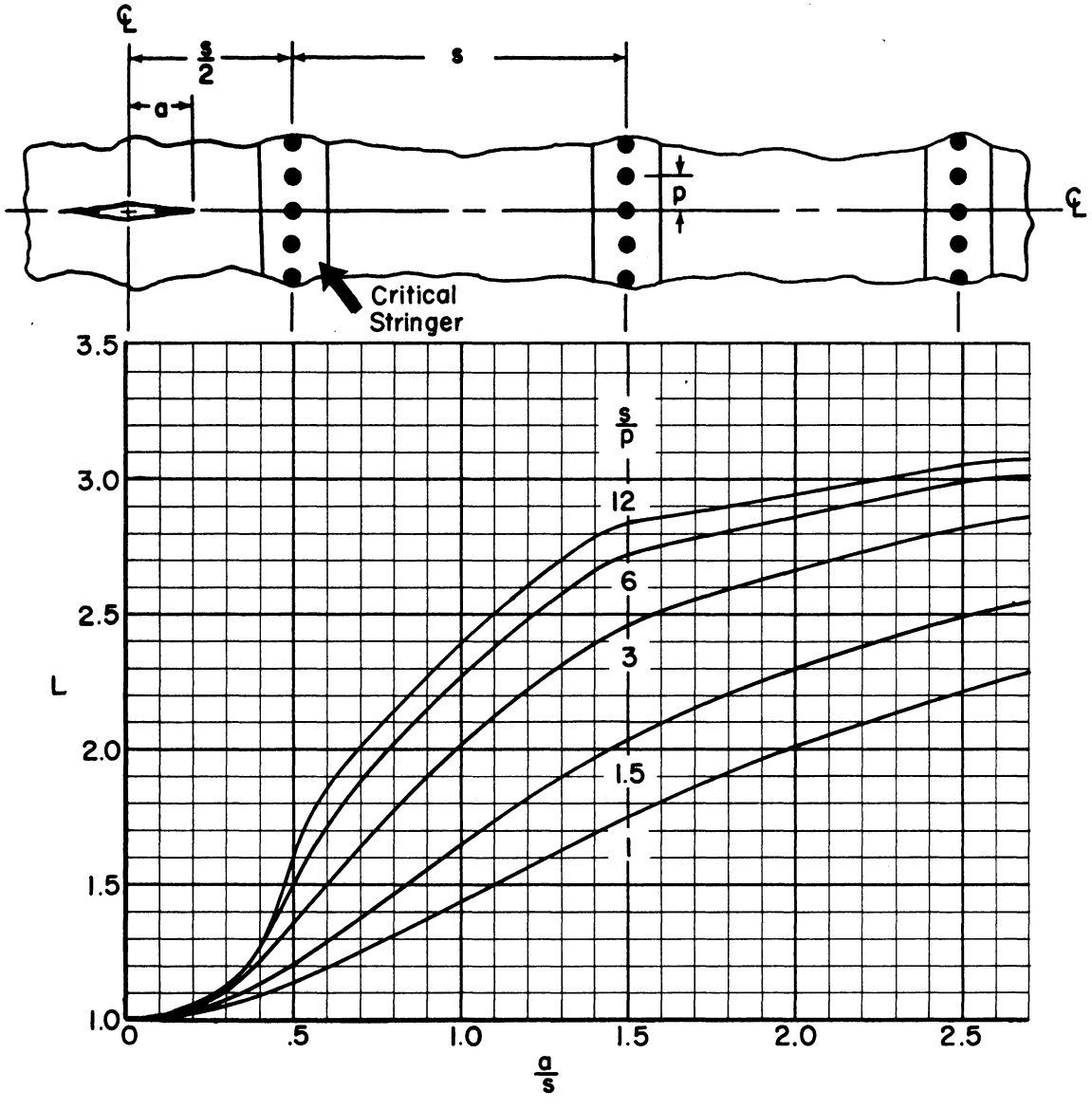

(b) 30 percent stiffening.

Figure 12.- Continued.

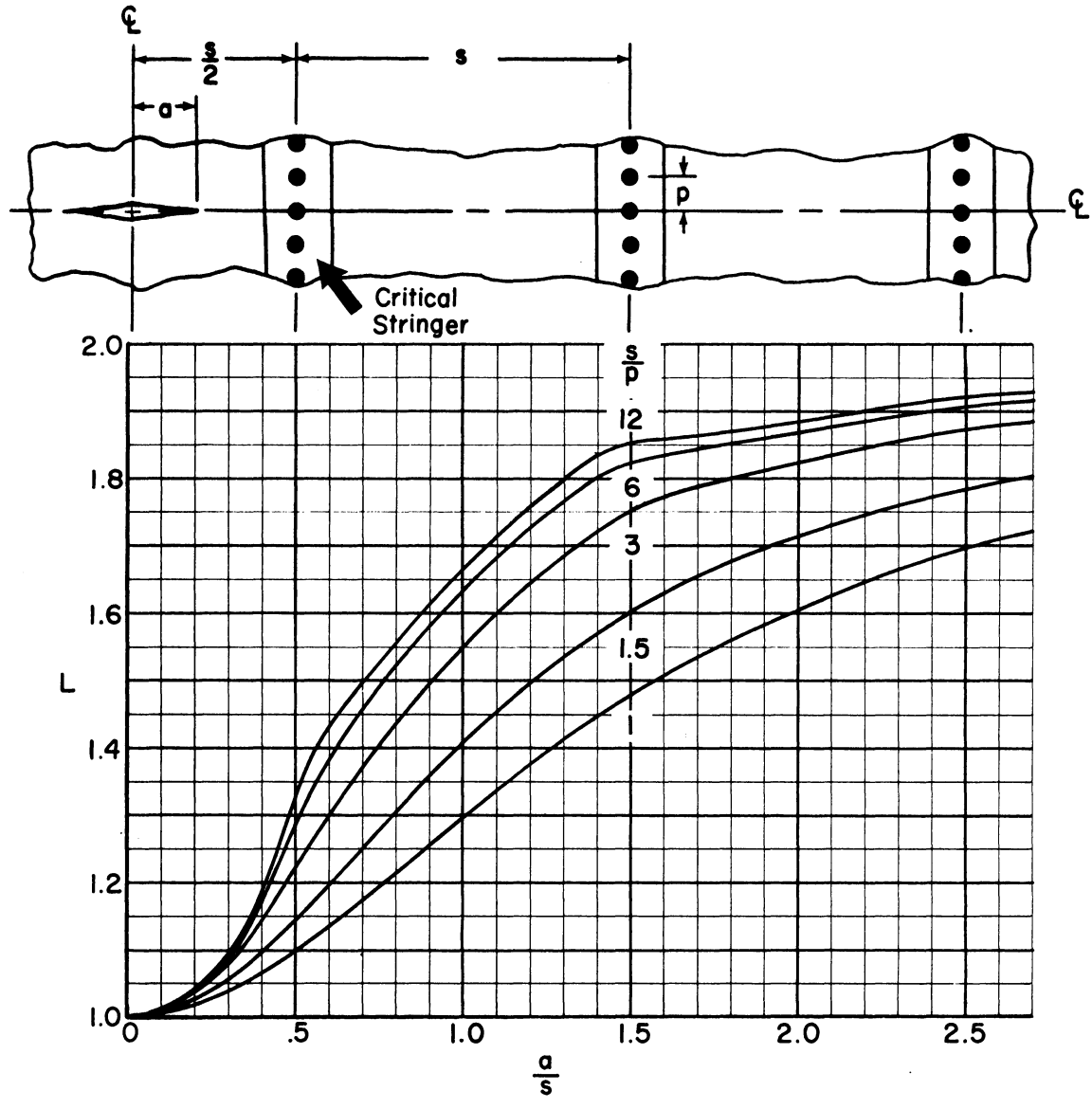

(c) 50 percent stiffening.

Figure 12.- Continued.

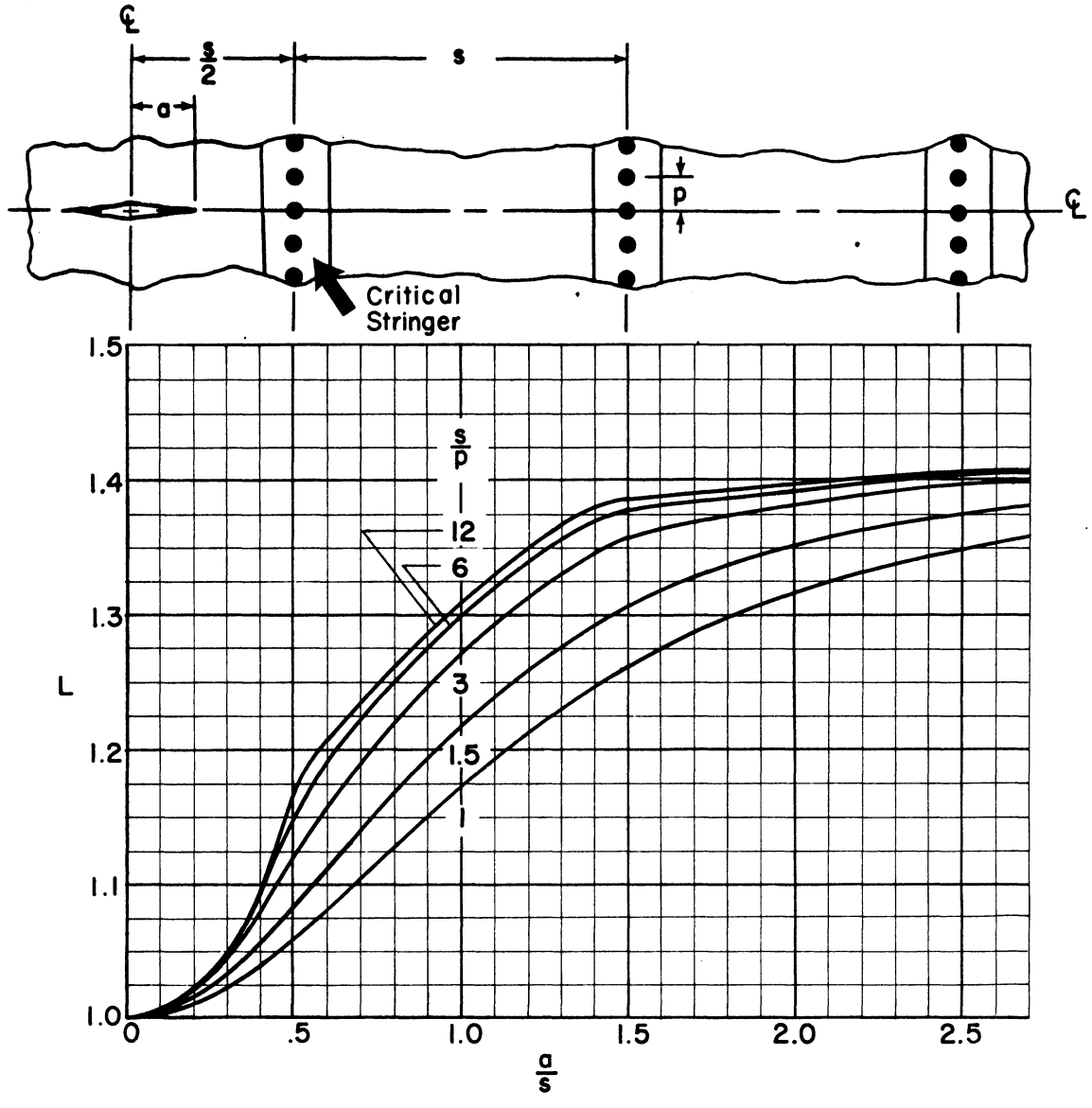

(d) 70 percent stiffening.

Figure 12.- Continued.

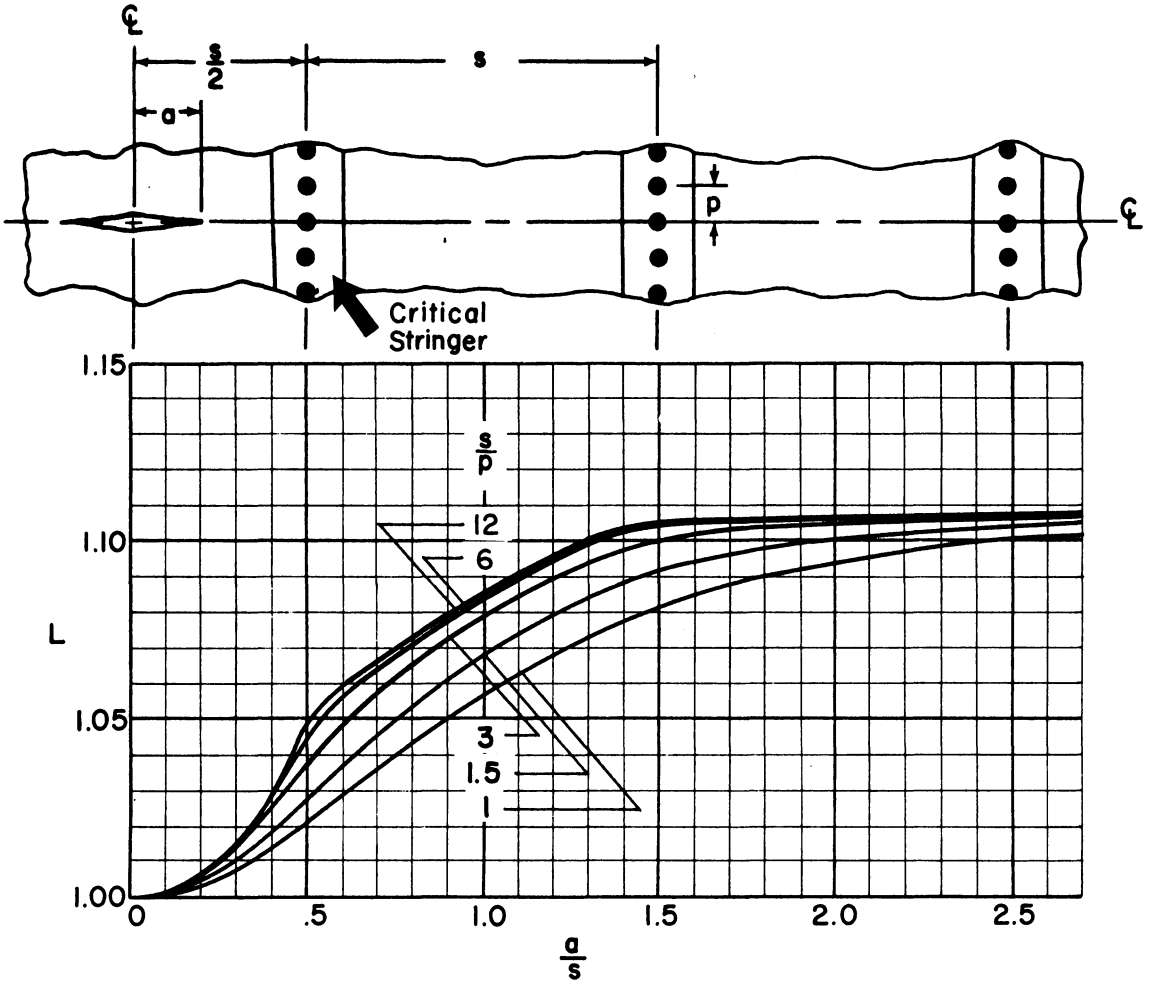

(e) 90 percent stiffening.

Figure 12.- Concluded.

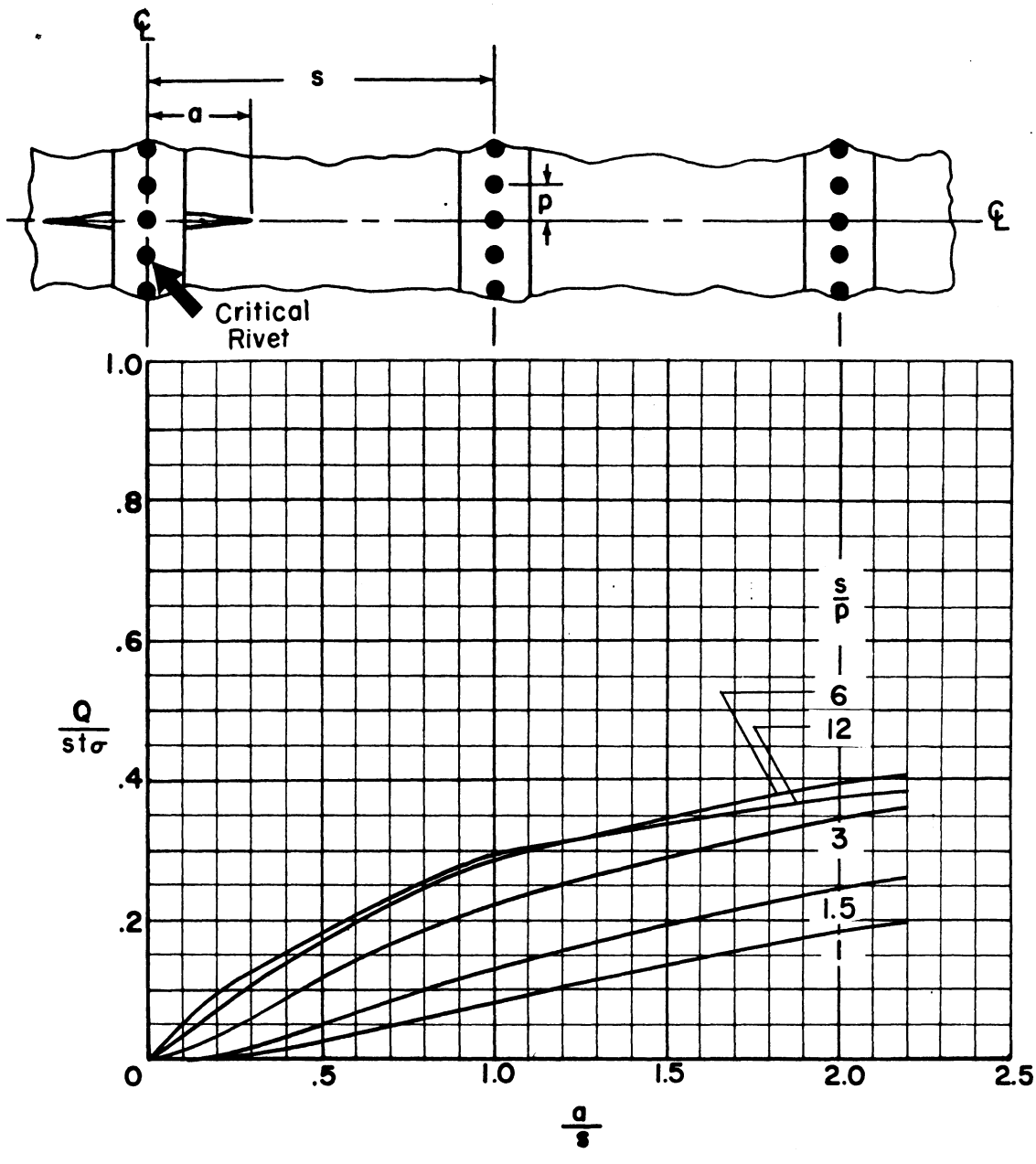

(a) 10 percent stiffening.

Figure 13.- Effect of crack length and rivet and stringer spacing on the force in the critical rivet. Crack initiating at a rivet.

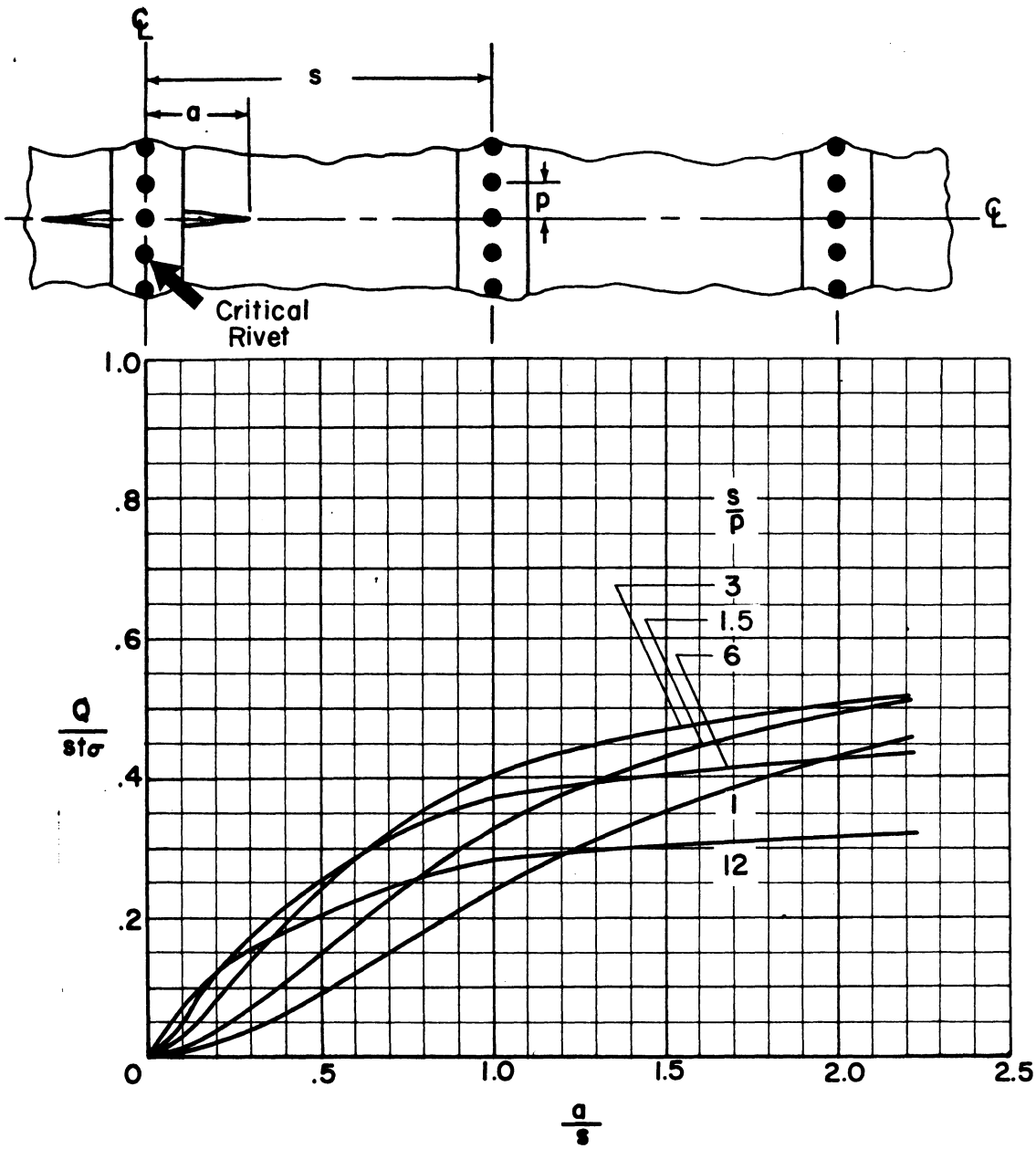

(b) 30 percent stiffening.

Figure 13.- Continued.

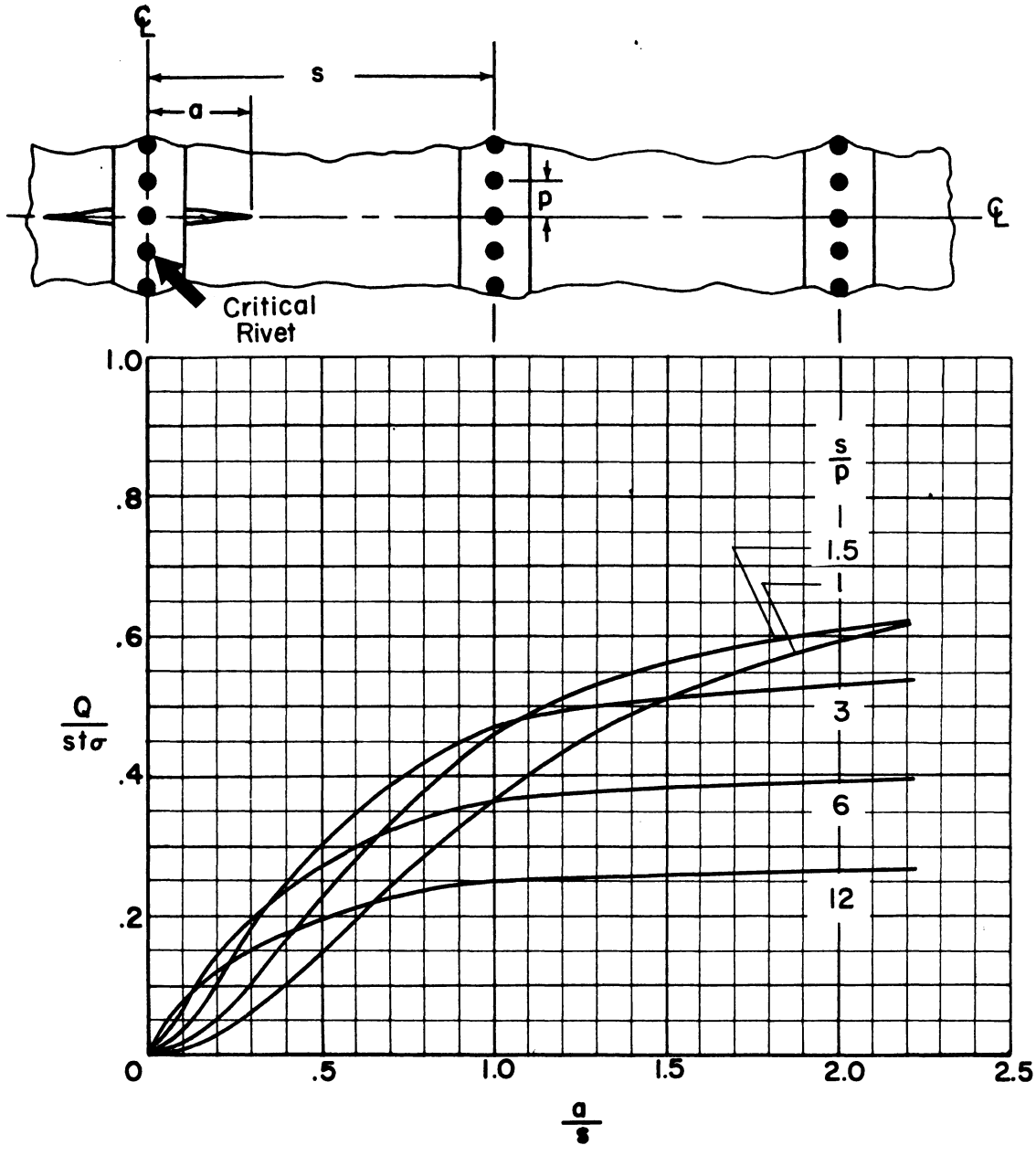

(c) 50 percent stiffening.

Figure 13.- Continued.

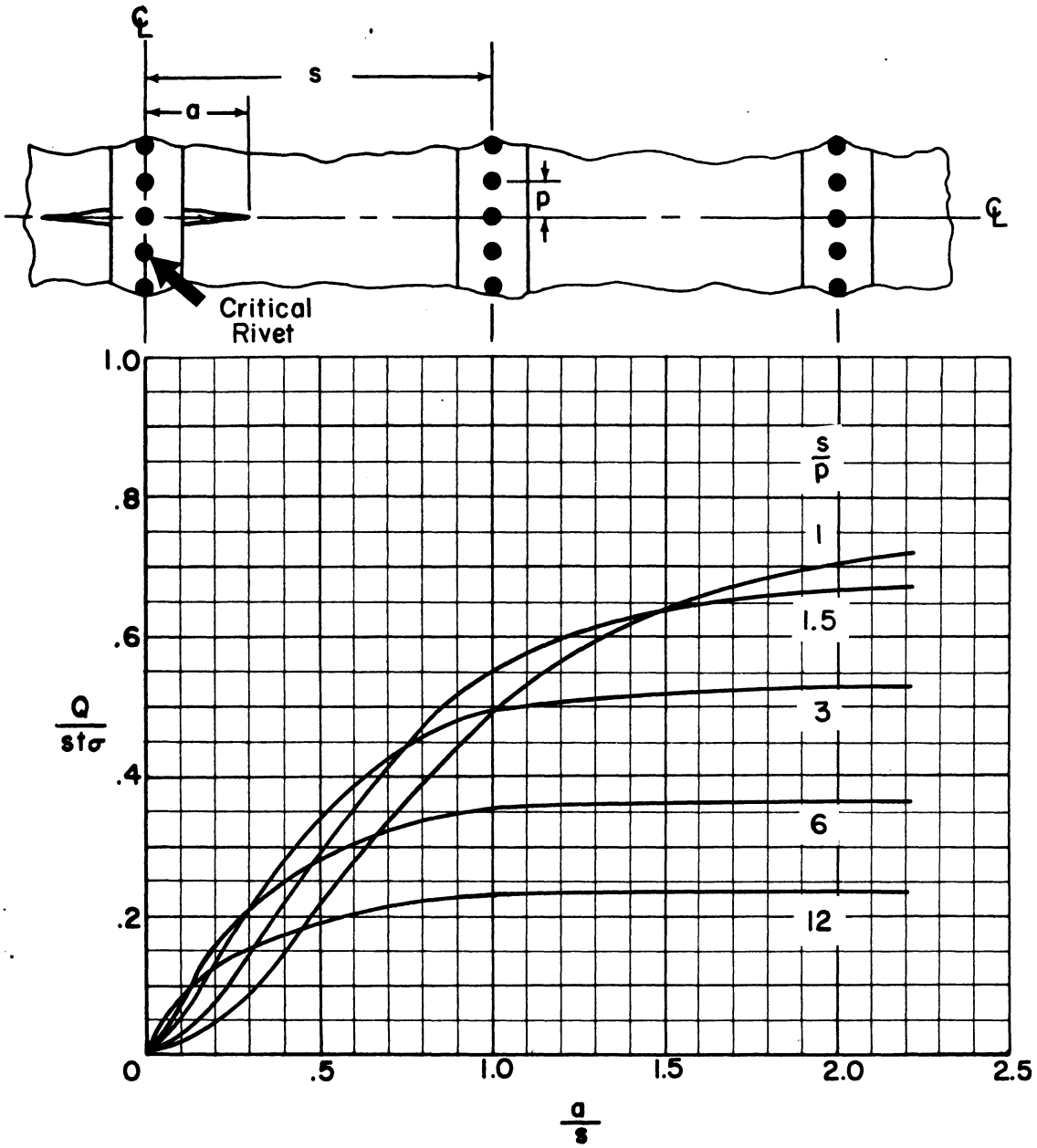

(d) 70 percent stiffening.

Figure 13.- Continued.

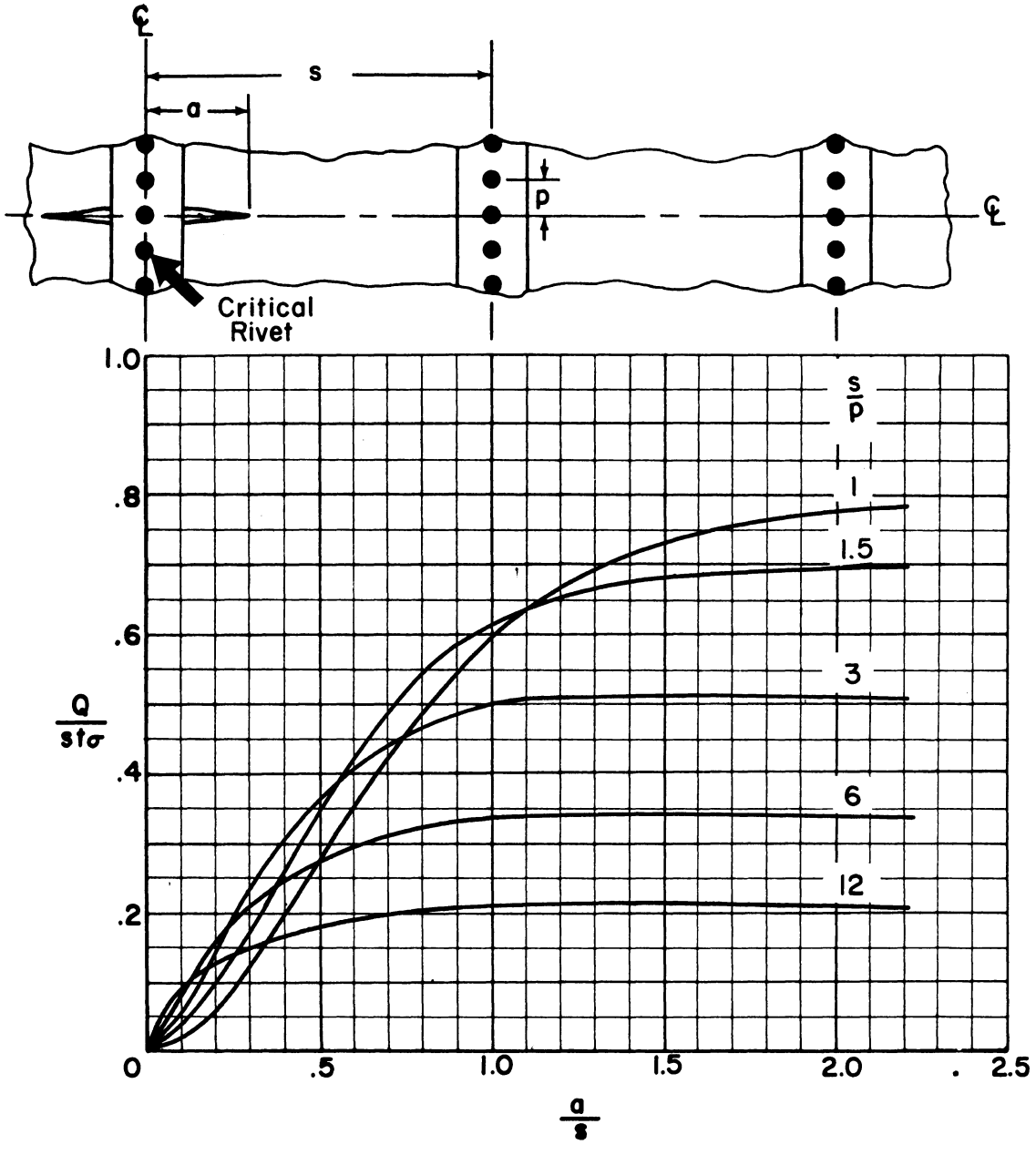

(e) 90 percent stiffening.

Figure 13.- Concluded.

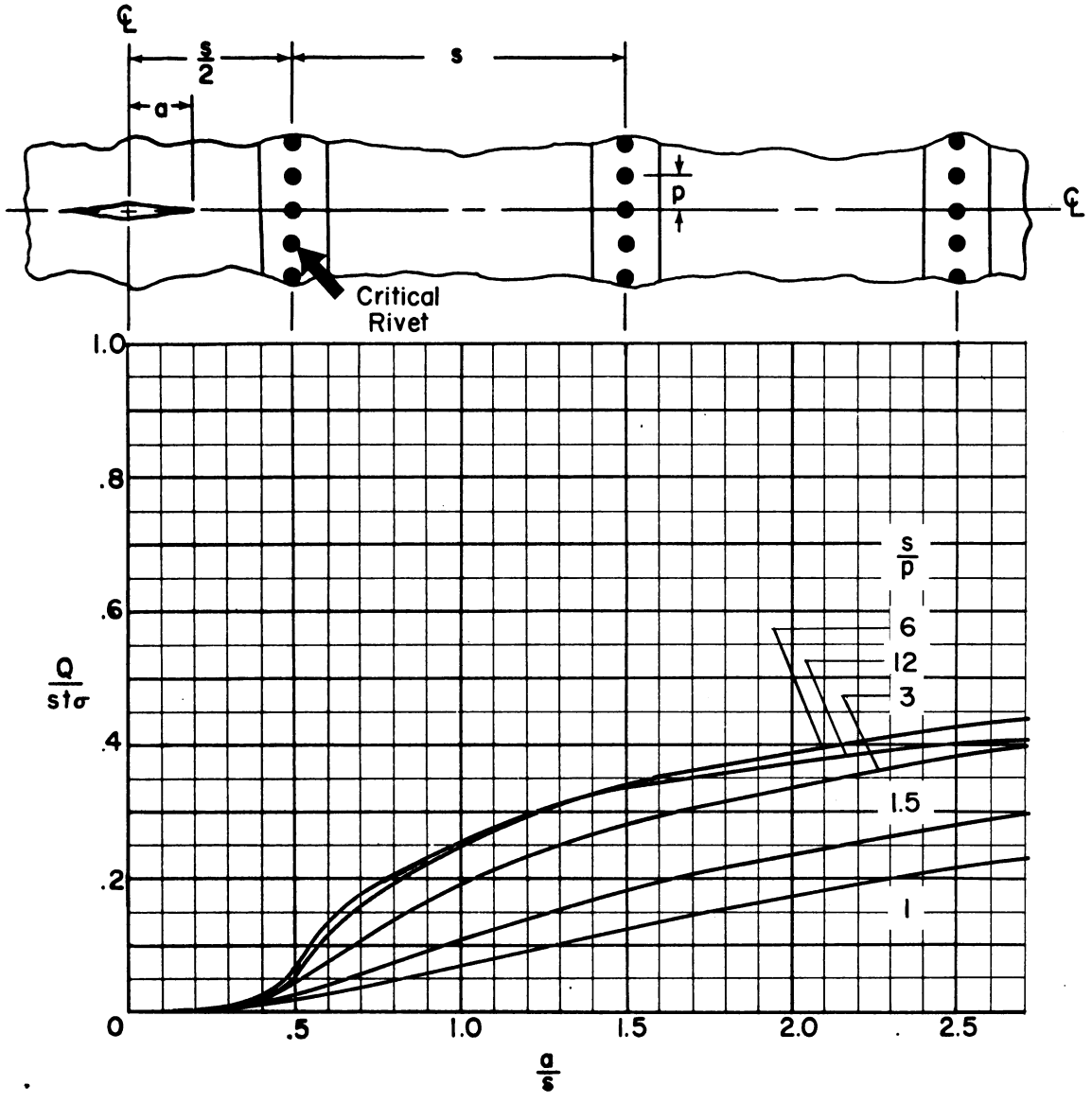

(a) 10 percent stiffening.

Figure 14.- Effect of crack length and rivet and stringer spacing on the force in the critical rivet. Crack initiating between stringers.

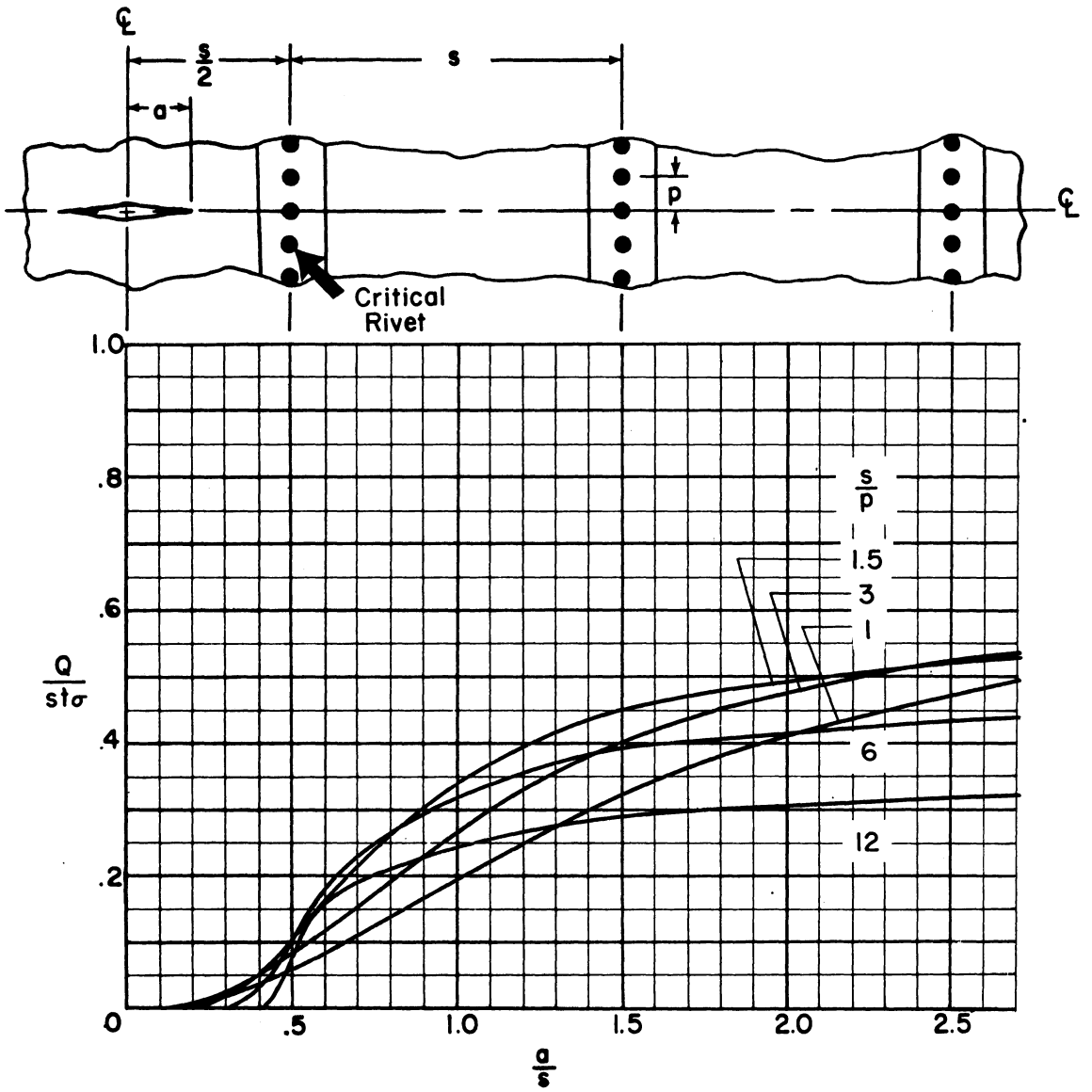

(b) 30 percent stiffening.

Figure 14.- Continued.

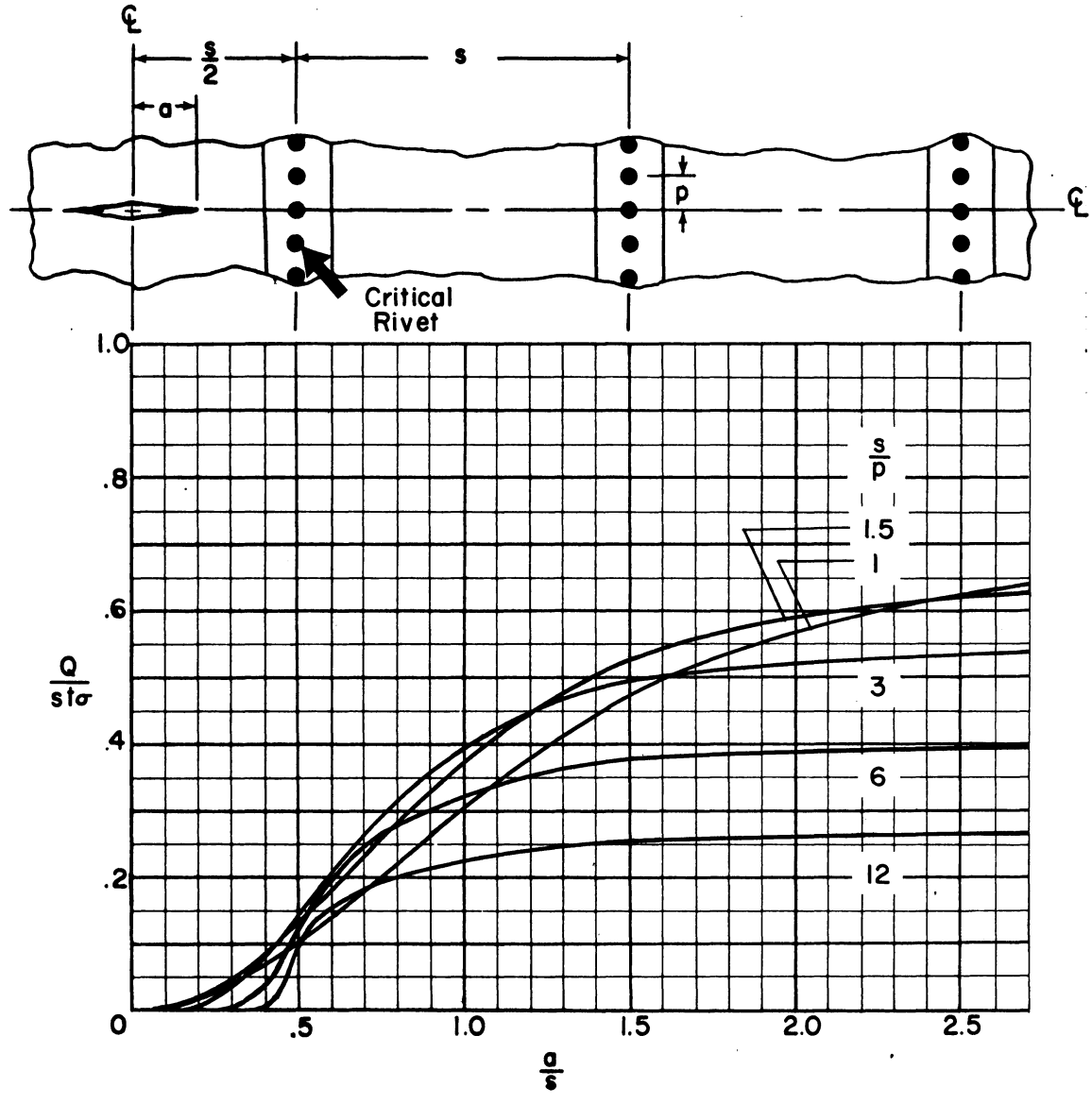

(c) 50 percent stiffening.

Figure 14.- Continued.

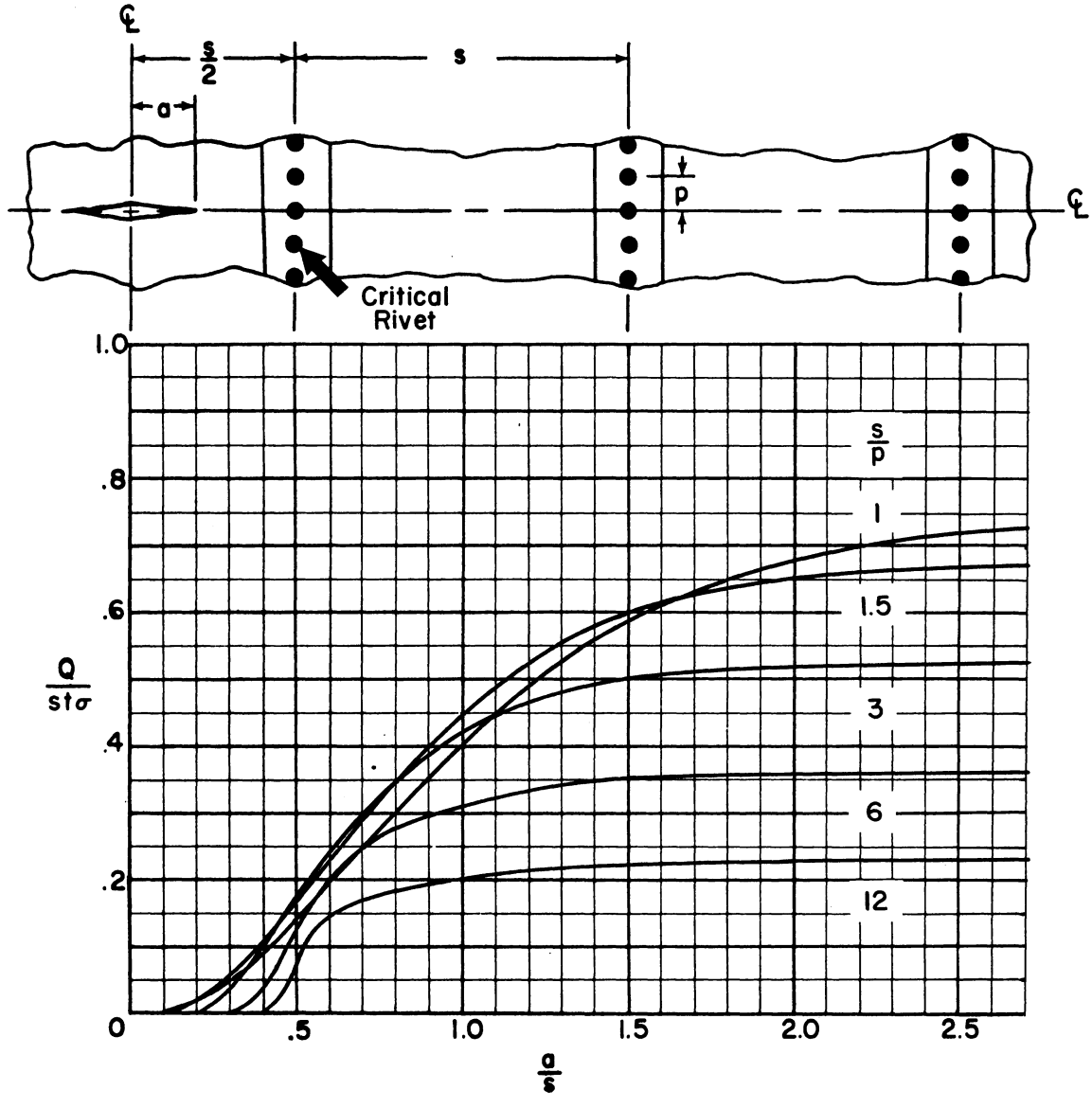

(d) 70 percent stiffening.

Figure 14.- Continued.

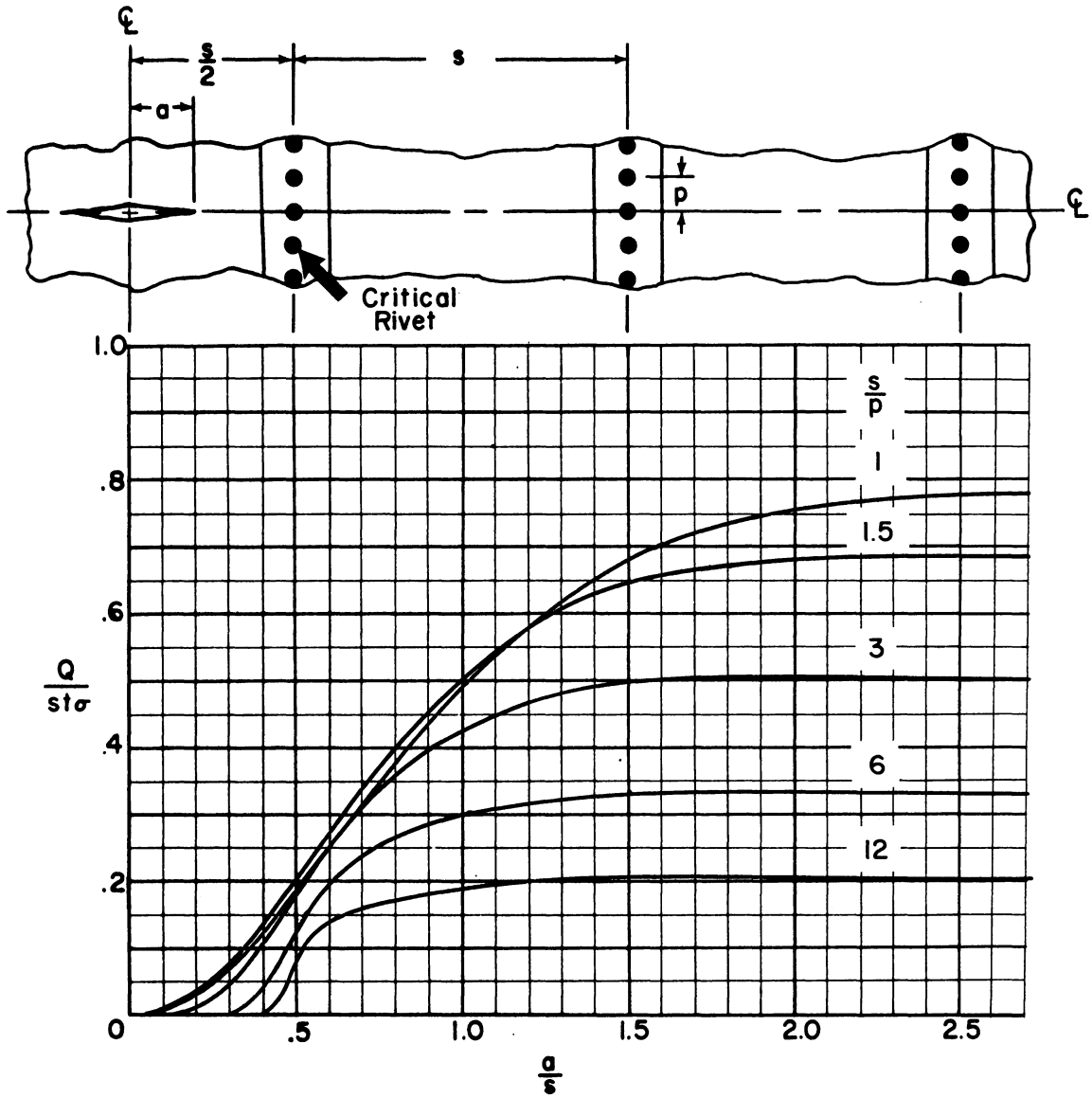

(e) 90 percent stiffening.

Figure 14.- Concluded.

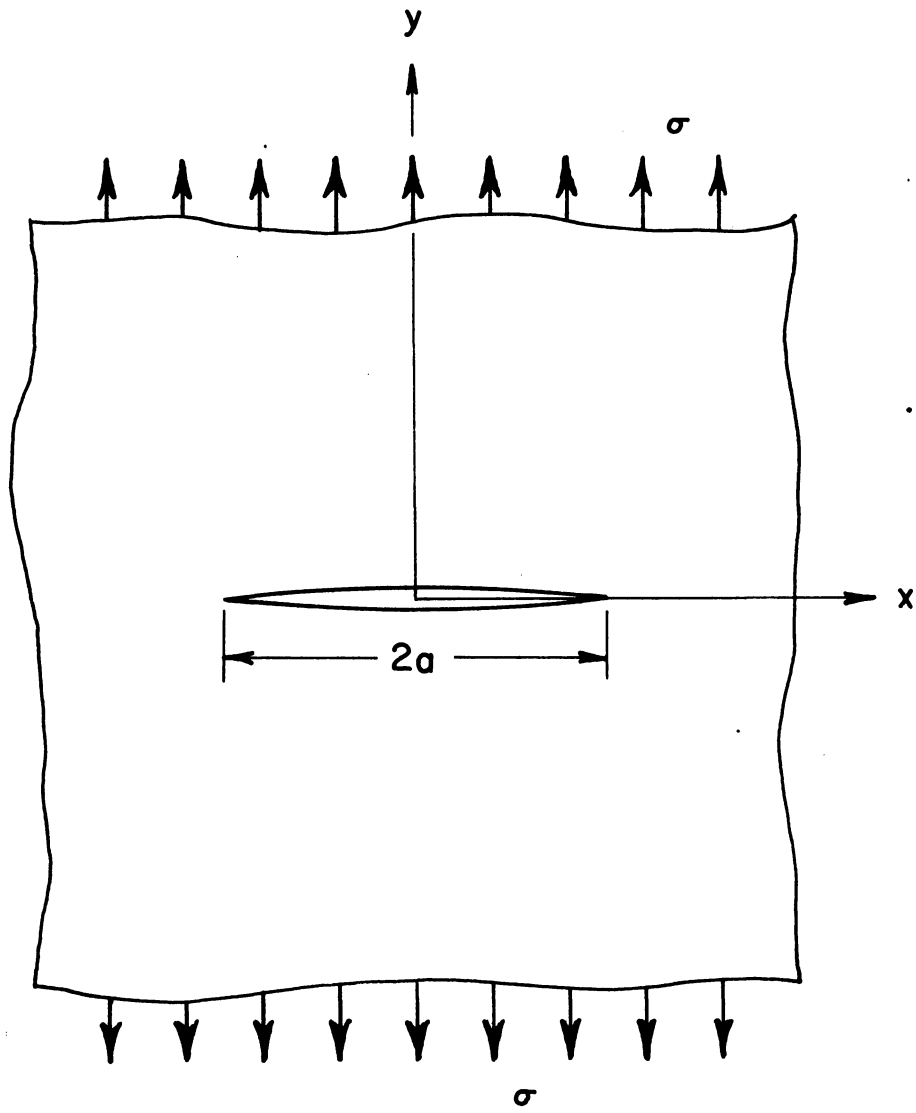

Figure 15.- Centrally cracked sheet with uniformly applied axial stress.

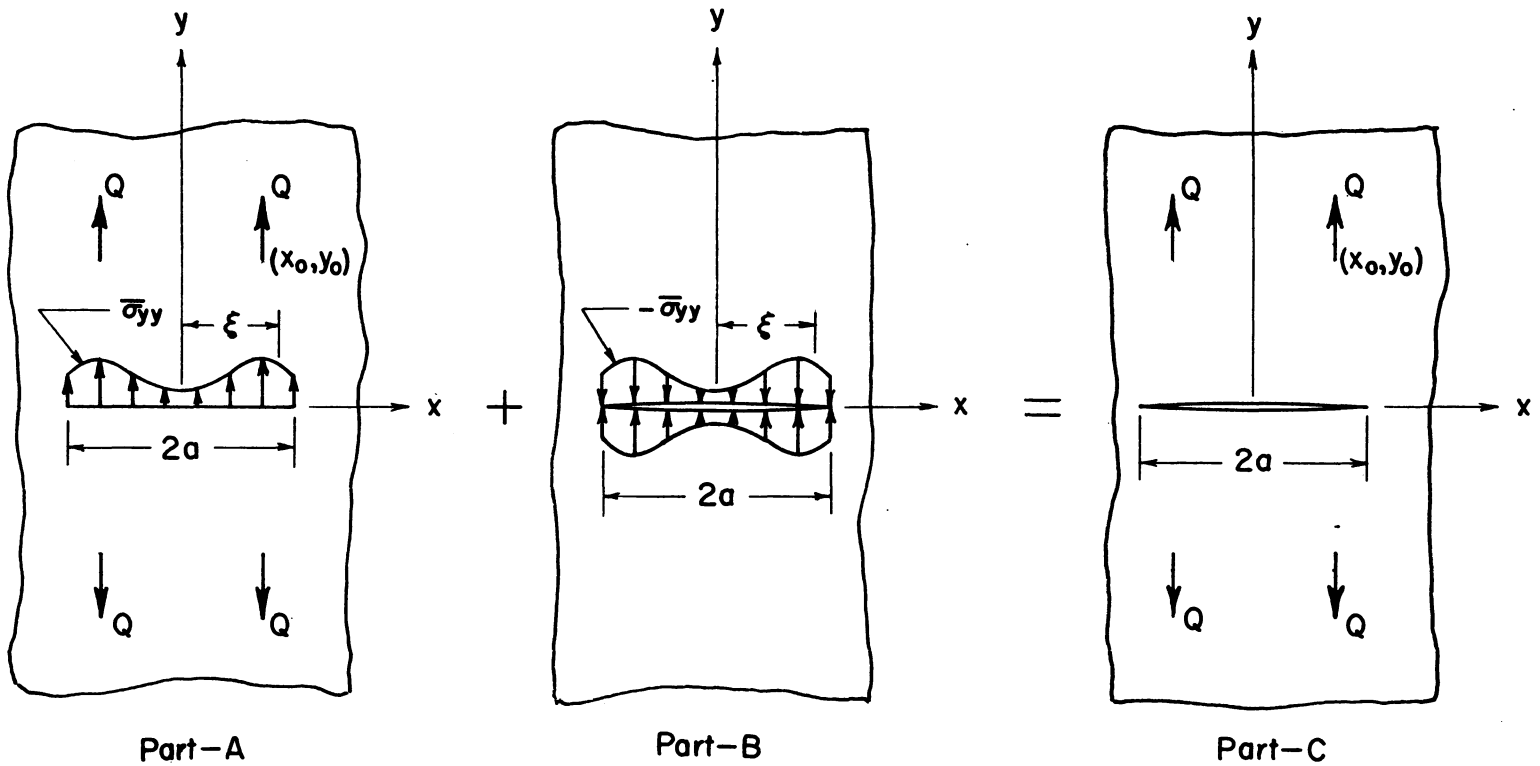

Figure 16.- Addition of solutions to obtain displacement field in cracked sheet with symmetrically applied point forces.

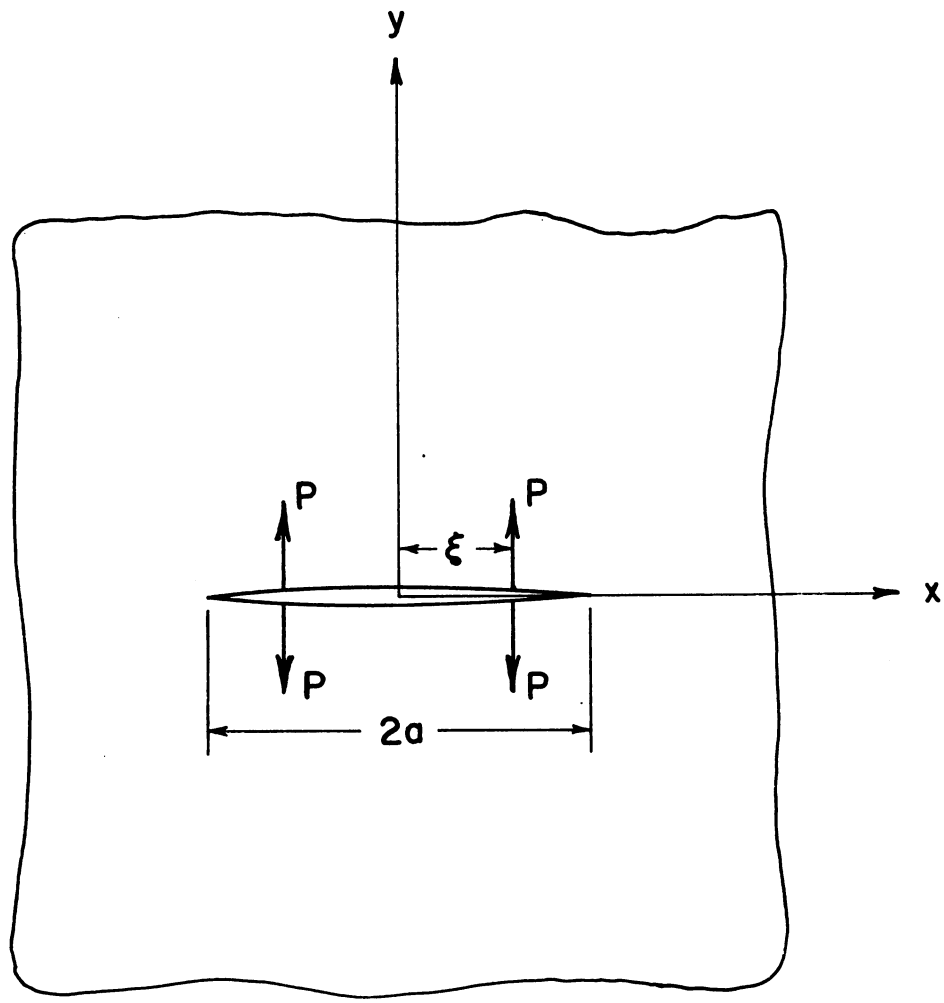

Figure 17. - Cracked sheet with wedging point forces applied symmetrically to the crack surfaces.

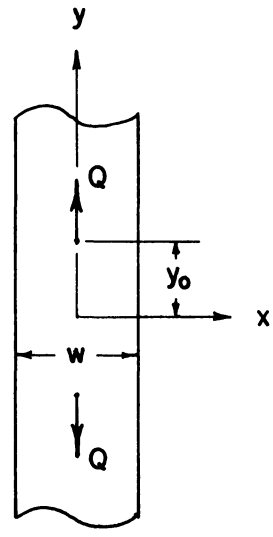

Boundary conditions

$\sigma_{xx} = \tau_{xy} = 0, \quad (\pm\frac{w}{2}, y)$

(a) Finite width stringer.

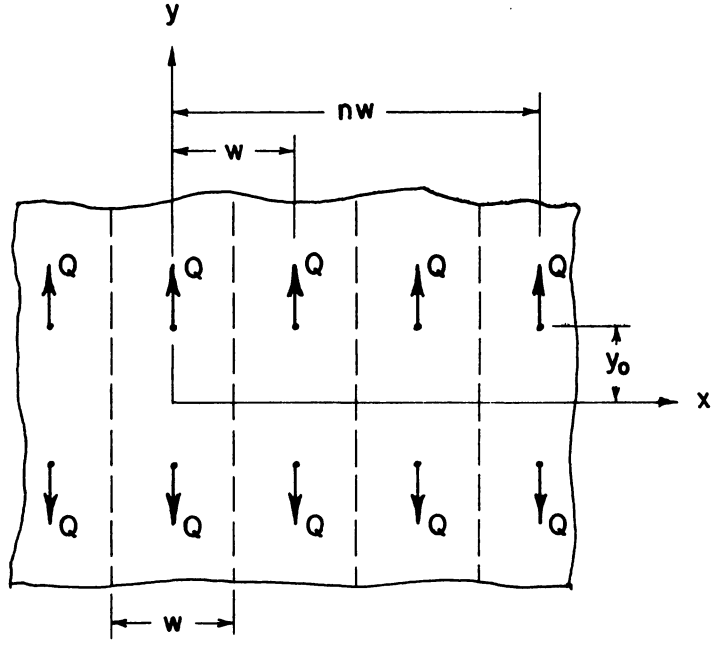

Boundary conditions

$\tau_{xy} = 0, \quad (\pm\frac{w}{2}, y)$

(b) Approximately finite width stringer.

Figure 18.- Stringer subjected to a pair of point forces.

THE EFFECT OF RIVETED AND UNIFORMLY SPACED STRINGERS ON THE STRESS INTENSITY FACTOR OF A CRACKED SHEET

By

Clarence C. Poe, Jr.

ABSTRACT

The effect of riveted and uniformly spaced stringers on the stress intensity factor of a centrally cracked sheet is determined. Also obtained is the force in the critical rivet and stringer. The results are presented for two symmetrical cases of crack location: the crack initiating at a rivet, and the crack initiating between two stringers.